Computation as a Tool for Glycogen Phosphorylase Inhibitor Design

Joseph M. Hayes*[,1] and Demetres D. Leonidas[2]

[1]*Institute of Organic & Pharmaceutical Chemistry, The National Hellenic Research Foundation, 48 Vassileos Constantinou Avenue, GR-116 35, Athens, Greece*

[2]*Department of Biochemistry and Biotechnology, University of Thessaly, 26 Ploutonos Str., 41221 Larissa, Greece*

Abstract: Glycogen phosphorylase is an important therapeutic target for the potential treatment of type 2 diabetes. The importance of computation in the search for potent, selective and drug-like glycogen phosphorylase inhibitors which may eventually lead to antihyperglycemic drugs is now firmly established. Acting solo or more effectively in combination with experiment in a multidisciplinary approach to structure based drug design, current day modeling methods are an effective means of reducing the time and money spent on costly experimental procedures. Glycogen phosphorylase is an allosteric protein with five different ligand binding sites, hence offering multiple opportunities for modulation of enzyme activity. However, the binding sites have their own individual characteristics, so that different modeling approaches may be more effective for each. This review is focused on advances in the modeling and design of new inhibitors of the enzyme aimed towards providing the reader with some useful hints towards more successful computer-aided inhibitor (drug) design targeting glycogen phosphorylase.

Keywords: Docking, free energy perturbation (FEP), glycogen phosphorylase, modeling, MM-GBSA, pharmacophore, QM/MM, QSAR.

Dedicated to the memory of our dear friend and colleague, Dr. Nikos G. Oikonomakos.

SECTION I: INTRODUCTION

Type 2 diabetes (T2D), characterised by insulin resistance and/or abnormal insulin secretion, affects approximately 150 million people worldwide and the prevalence is expected to double by the year 2025 [1]. Current treatments have several side effects, the potential to cause hypoglycemia and are inadequate for 30-40 % of patients [2, 3]. Insulin malfunction in the liver leads to an increase in hepatic glucose production and is the main contributor to high blood glucose levels. Glycogenolysis may account for more than 70 % of the hepatic glucose production, and a substantial portion of glucose formed by gluconeogenesis is cycled through the glycogen pool [4, 5]. The main regulatory enzyme of glycogenolysis is glycogen phosphorylase (GP) which catalyses the breakdown of glycogen to glucose-1-phosphate (Glc-1-P) which is eventually converted to glucose [6, 7]. Inhibition of hepatic GP could suppress glucose production arising from both glycogenolysis and gluconeogenesis, and hence is a promising therapeutic target for the treatment of T2D [8, 9].

GP exists as a dimer (EC 2.4.1.1; MW ~ 97500 Da; 842 residues) and in two interconvertible forms: GPa (phosphorylated form, high activity and substrate affinity, predominantly active R state) and GPb (unphosphorylated form, low activity and substrate affinity, predominantly inactive T state). The structures of T and R state GP have been characterized; X-ray diffraction studies have shown the conformational changes that take place following activation of the muscle enzyme and its conversion from the T to R state by phosphorylation or AMP [10-13]. It is a typical allosteric enzyme with five different binding sites identified to date: the catalytic, inhibitor, allosteric, new allosteric and glycogen storage sites (Fig. (**1**)). Progress in the prediction and design of new GP inhibitors (GPIs) binding at these sites [9, 14, 15] has been accelerated by the availability of many high resolution co-crystallized GP-inhibitor complexes. The knowledge of the three-dimensional structures of protein-ligand complexes reveals the receptor-ligand interactions critical to ligand recognition and with that facilitates structure-based drug design (SBDD). Computation provides an efficient tool towards exploiting the known structural data in the design and proposal of new inhibitors for experimental evaluation. Two recent review articles have focused on the experimental aspects of the design of new GPIs [14, 15], one of them also containing a review of the related computational work [14]. A general review of modeling studies on different targets for T2D has also been published [16]. This review focuses on GP and inhibitor design from a modeling perspective, highlighting based on recent computational work how calculations can support experiment in a more rational and time-efficient approach to design of potent, drug-like GPIs. Section II highlights important information regarding the binding features at each site; section III analyses the computational methods which can be applied to model inhibitor binding properties *versus* their computational expense; section IV reviews previous modeling studies on GPIs exploiting these methods; while section V examines *in silico* approaches to the design of more drug-like GPIs.

*Address correspondence to this author at the Institute of Organic & Pharmaceutical Chemistry, The National Hellenic Research Foundation, 48 Vassileos Constantinou Avenue, GR-116 35, Athens, Greece;
Tel: +30 210 727 3856; Fax: +30 210 727 3831; E-mail: jhayes@eie.gr

1389-5575/10 $55.00+.00

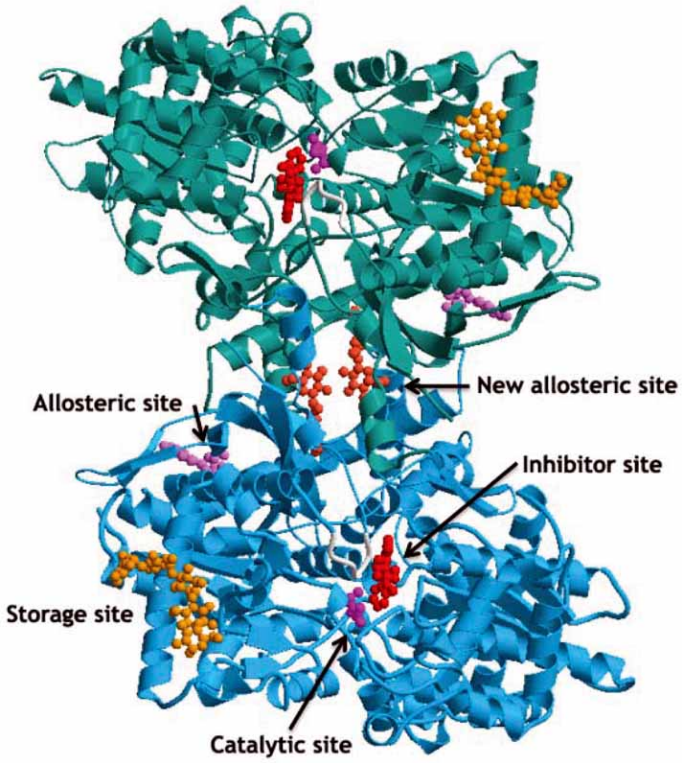

Fig. (1). A schematic diagram of the muscle GPb dimeric molecule viewed down the 2-fold. The positions of the catalytic, allosteric, inhibitor, glycogen storage and new allosteric sites are shown. The catalytic site, which includes the essential cofactor pyridoxal 5'-phosphate (PLP, not shown), is buried at the centre of the subunit accessible to the bulk solvent through a 15 Å long channel. Glucose (shown in purple), a competitive inhibitor of the enzyme that promotes the less active T state through stabilization of the closed position of the 280s loop (shown in white), binds at this site. The allosteric site, which binds the activator AMP, other phosphorylated compounds such as ATP, glucose-6-P, and the Bayer compound W1807 (shown in magenta), is situated at the subunit-subunit interface some 30 Å from the catalytic site. The inhibitor site, which binds purine compounds, such as caffeine, nucleosides or nucleotides at high concentrations, and flavopiridol (shown in red) is located on the surface of the enzyme some 12 Å from the catalytic site and, in the T state, obstructs the entrance to the catalytic site tunnel. The new allosteric inhibitor site, located inside the central cavity formed on association of the two subunits, binds CP320626 (shown in orange) and is some 15 Å from the allosteric effector site, 33 Å from the catalytic site and 37 Å from the inhibitor site. The glycogen storage site is indicated by maltoheptaose (shown in yellow).

SECTION II: TARGETING GP BINDING SITES

Critical to effective structure based drug (inhibitor) design of GPIs targeting the different binding sites is knowledge of the binding site features such as key binding site residues, site flexibility, solvent exposure and hydrophobicity.

Catalytic Site

The GP catalytic site includes the essential cofactor pyridoxal-5'-phosphate (PLP) and is buried at the center of the GP monomer subunit accessible to bulk solvent through a 15 Å long channel. Catalytic site GPIs promote the T state (less active) conformation through stabilisation of the closed position of 280s (residues 282-287) loop and block access of the substrate glycogen to the catalytic site. α-D-glucose (**1**) is the physiological inhibitor of the GP catalytic site with a K_i of 1.7 mM for RMGPb inhibition; β-D-glucose (**2**) binds with a K_i of 7.4 mM [17]. Design of inhibitors for this site have therefore initially focused on glucose based analogues (**3**) with α- and β-substitutions at the anomeric C1 atom, with the β-substitutions aiming to exploit the catalytic subsite called β-cavity, an empty space at the β-1-C configuration lined by both polar and non-polar groups. Given the location of the catalytic site, the GP monomer structure is sufficient for modeling GPI binding at this site. The glucopyranosylidene-spiro-isoxazoline (**4**(R=naphthyl)) shown bound at the catalytic site of GPb (PDB code 2QRP; Fig. (**2**)) is one of the most potent GPIs identified at this site to date with a K_i for RMGPb inhibition of 630 nM [18]. An interaction that is often pursued in catalytic site GPI design is a hydrogen bond from inhibitor to the main chain O of His377. For example, N-Acetyl-β-D-glucopyranosylamine (NAG (**5**)) which forms a hydrogen bond from NH of the ligand to His 377 O inhibits RMGPb with a K_i of 32 μM [19], approximately 50 times better than α-D-glucose (**1**) and binds to the enzyme without any significant structural conformational changes within the catalytic site; residues of the 280s loop are stabilized in the same conformation observed in the RMGPb – α-D-glucose complex.

Some ligands (e.g. *N*-acyl-*N*'-β-D-glucopyranosyl ureas ligands) (**6**) [14, 20] upon binding to the catalytic site induce (varying) shifts of the 280s loop at the catalytic site. Depending on the degree of shift involved, this may require consideration in modeling studies (*vide infra*). Two different

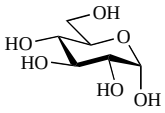

1
a-D-glucose
Ki (RMGPb) = 1.7 mM [17]

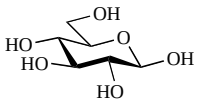

2
β-D-glucose
Ki (RMGPb) = 7.4 mM [17]

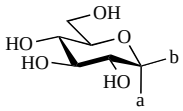

3
glucose analogue

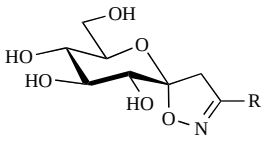

R =

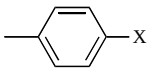

X	Ki (μM; RMGPb) [18]
OMe	6.6
Me	7.9
H	19.6
NO_2	92.5

R =

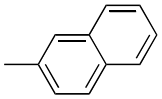

Ki (RMGPb) = 630 nM [18]

4
glucopyranosylidene-spiro-isoxazolines

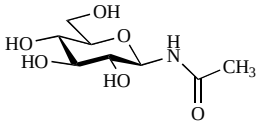

5
NAG
Ki (RMGPb) = 32 μM [19]

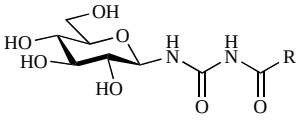

R =

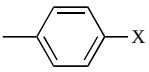

X	Ki (μM; RMGPb) [14]
H	4.6
CF3	1.8
$C(CH_3)_3$	0.7

R	Ki (μM; RMGPb) [14]
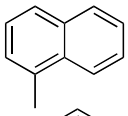	15
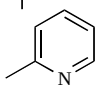	68
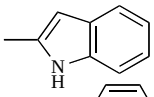	4.0
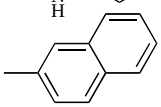	0.35

6
N-acyl-N'-β-D-glucopyranosyl ureas

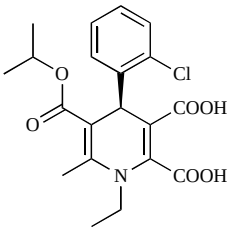

7
Bayer W1807
Ki = 1.6 nM (GPb);
10.8 nM (GPa) [32]

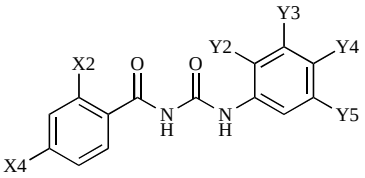

acyl ureas (**8**)

8a: X2=Y3=Cl;Y4=O$(CH_2)_5$COOH;X4=Y2=Y5=H
IC_{50} (HLGPa) = 2 μM; IC_{50} (RMGPb) = 2.2 μM [26]
8b: X2=Cl; X4=F; Y2=OMe; Y3=Y4=H; Y5=OH
IC_{50} (HLGPa) = 23 nM [26]
8c: X2=Cl;X4=X5=F;Y2=OMe;Y3=Y4=H;Y5=NHCONHMe
IC_{50} (HLGPa) = 53 nM [26]

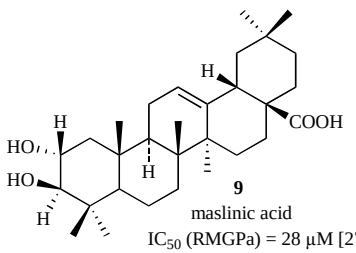

9
maslinic acid
IC_{50} (RMGPa) = 28 μM [27]

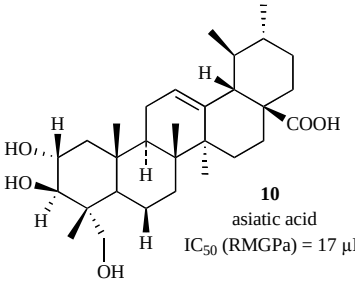

10
asiatic acid
IC_{50} (RMGPa) = 17 μM [27]

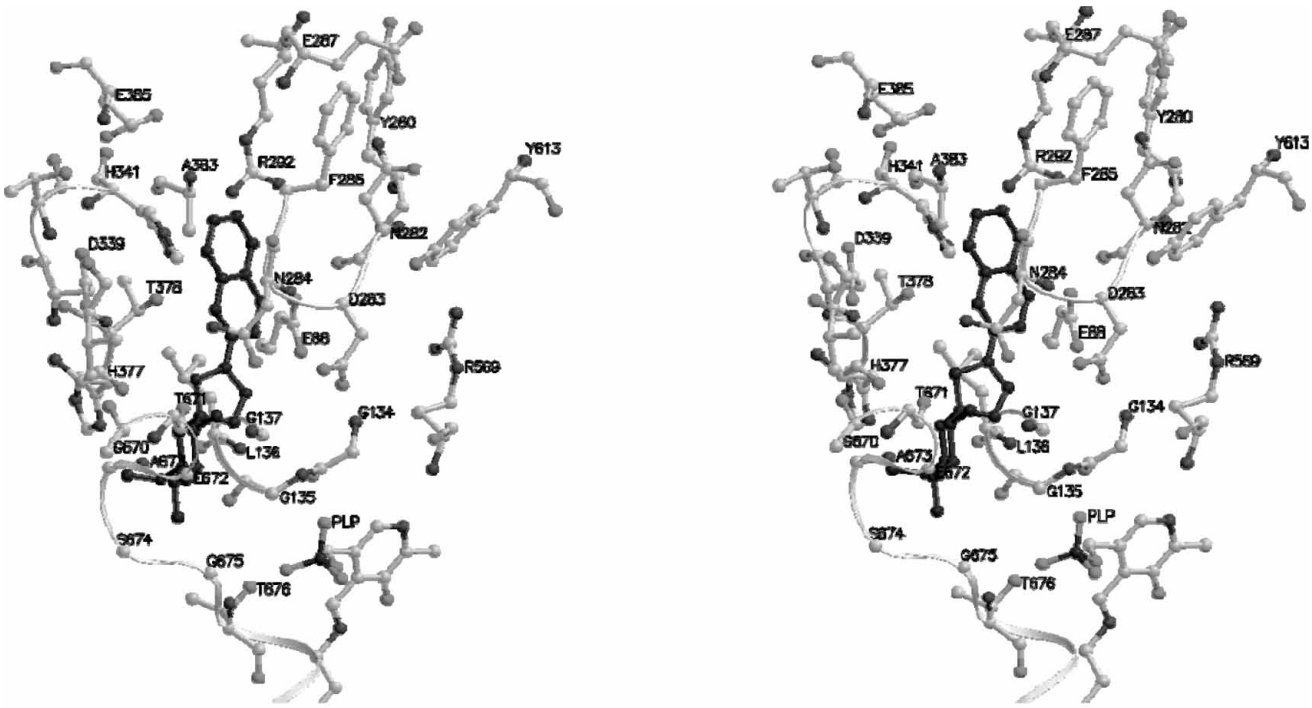

Fig. (2). The glucopyranosylidene-spiro-isoxazoline derivative **4** (R=naphthyl) shown bound at the catalytic site of GPb (PDB code 2QRP) [18], blocking access of the substrate (glycogen) to the site. The inhibitor on binding stabilizes the T state of the enzyme with the 280s loop in the closed position. A large number of residues can contribute to binding at this site, as indicated, with the β-channel lined by both polar and non-polar groups. Inhibitor dependent structural rearrangements at the site (as outlined in the text) are often required to accomodate inhibitors (most frequently in 280s loop), as are water-bridging interactions [14]. All such interactions accumulate to define the overall binding affinity of a GPI.

conformations of Asn284 [21], the position of phosphate group of PLP [21], conformation of the Asp283 sidechain carboxylate [21, 22], and even orientations of Ser674 [21] and His377 backbones [21, 23] are dependant on the structure of bound inhibitor. These and other importance shifts in the Ala673-Thr676 sequence, 280s and 380s (residues 377-384) loops are also highlighted in reference [24].

Allosteric Site

The allosteric (AMP binding) site is situated at the subunit – subunit interface approximately 30 Å from the catalytic site and is partially exposed to the solvent. This site recognizes a variety of phosphorylated compounds such as IMP (weak activator), ATP, glucose-6-P (Glc-6-P), NADH, UDP-glucose, 2-deoxy-glucose-6-P, β-glycerophosphate, and inorganic phosphate [8]. It also binds allosteric inhibitors such as the Bayer compound W1807 (**7**) [25], acyl ureas (e.g. **8a**-**8c** [26]), triterpenes (e.g. maslinic **9** and asiatic acid **10** [27]) and the GlaxoSmithKline series of anthranilimide GPIs (e.g.: **11** and **12** [28]). Features for binding of W1807 (PDB code 3AMV) at the site are shown in Fig. (**3**). The inhibitors at the site work by either direct inhibition of AMP binding and/or indirect inhibition of substrate binding through stabilization of the T- or T'-state conformation, with the superscript prime referring to the symmetry related monomer subunit. Allosteric activators, such as AMP or allosteric inhibitors such as ATP and Glc-6-P, can alter the equilibrium between a less active T state and a more active R state or *vice versa*, according to the Monod-Wyman-Changeux model for allosteric proteins [29].

W1807 is the most potent inhibitor of GP known to date (K_i =1.6 nM for GPb and K_i =10.8 nM for GPa) and acts in synergy with both glucose and caffeine. It exhibits blood glucose lowering effects in rats [30] and reduces glycogenolysis both by inactivation and by inhibition of residual GPa [31]. The interactions between W1807 and RMGPa are dominated by charge-charge interactions between the carboxylate groups and the arginine residues, and by three major groups of non-polar contacts (Fig. (**3**)). Binding of W1807 in the T-state GPb crystals is accompanied by substantial conformational changes. Residues 43′ to 49′ move closer to the other subunit and tighten the W1807 site, while residues 192 to 196 shift to contribute (through Phe196) van der Waals interactions. These shifts appear important in stabilizing the T state. The shifts in the region of 43′ to 49′ and 192 to 196 affect residues remote from the allosteric site (such as Pro194), which in turn affect the subunit/subunit interface packing [32]. The enzyme shows a small rotation (1.6°) and this rotation bringing the two subunits of the dimer closer together. The conformational changes induced on binding W1807 are almost identical to those that accompany the binding of the Glc-6-P. Glc-6-P binds at the allosteric site and promotes conformational changes in the T-state GPb [33]. However, there are significant differences in the type of contacts made by Glc-6-P and W1807 at the allosteric site.

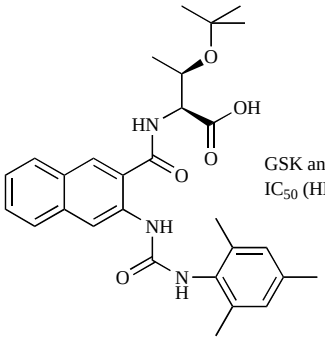

11
GSK anthranilimide
IC_{50} (HLGPa) = 7 nM [28]

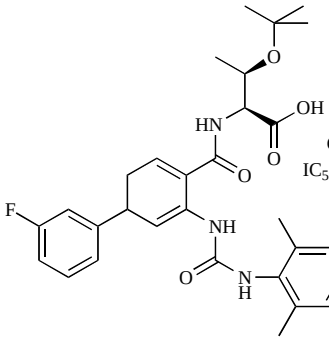

12
GSK anthranilimide
IC_{50}(HLGPa) = 3 nM[28]

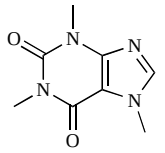

13
caffeine
Ki = 0.1 mM (RMGPa) [36]
Ki = 0.08 mM (RMGPb) [37]

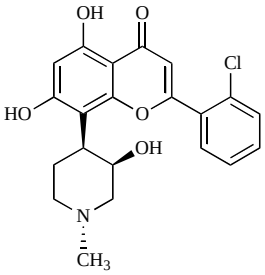

14
flavopiridol
Ki (RMGPb) = 1.16 μM [14]

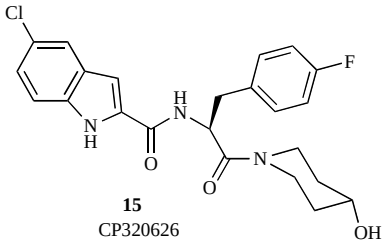

15
CP320626
IC_{50} = 0.2 μM (HLGPa);
0.083 μM (HMGPa) [40]

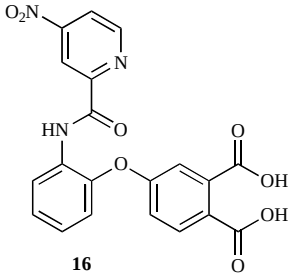

16
phenyl-diacid
IC_{50} (HLGP)= 1 nM;
IC_{50} (HMGP) = 3 nM[48]

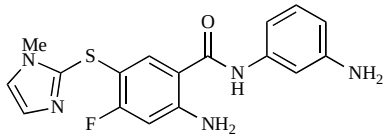

17
benzamide derivative
IC_{50} = 2.68 μM (RMGPa) [44]

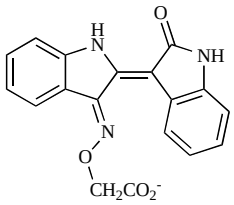

18
E243
Ki = 21 μM (RMGPb) [52]

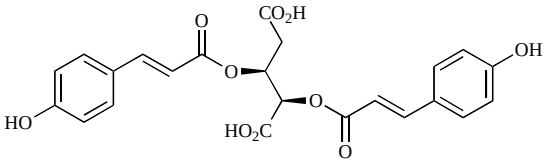

19
FR258900
IC_{50} = 2.5 μM (HLGPa) [53]
Ki = 0.46 μM (RMGPb) [54]

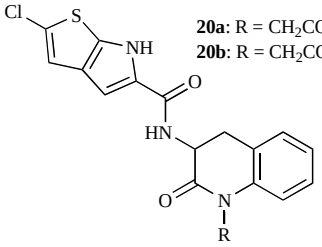

20a: R = CH_2CONH_2
20b: R = $CH_2CONH(CH_2)_2OH$

20
AstrazZeneca
IC_{50} (**20a**) = 135 nM (GPa) [55]
IC_{50} (**20b**) = 121 nM (GPa) [55]

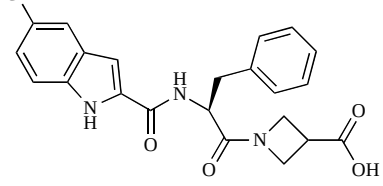

21
CP403700
IC_{50} = 0.045 μM (HLGPa) [59]

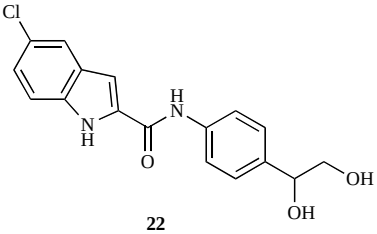

22
Astellas Pharma
IC_{50} = 0.90 μM (HLGPa) [41]

Contacts from Glc-6-P to the enzyme are mostly hydrogen-bonding interactions and there are relatively few van der Waals interactions. In contrast, the contacts from W1807 to GPb are dominated by the non-polar van der Waals interactions and by ionic interactions to arginine residues. The non-polar contacts appear to be the major source of binding energy that results in an inhibitor with nM affinity compared with the μM affinity exhibited by Glc-6-P.

For binding of GlaxoSmithKline compound **11**, the naphthalene group binds in a narrow lipophilic channel close to the solvent exposure [28]. Inhibitor dependent conformational changes have also been observed; for binding of **11**, Arg193 adopts a conformation suitable for π-stacking interactions [28] which is different to that observed for other allosteric site GPIs [26, 34]. It has also been reported that Arg309 adopts a conformation that is flipped away from the binding site and does not engage in hydrogen bond interactions [28, 34]. Such input from the available structural data is crucial to modeling more accurately the binding of new inhibitors. The different binding modes and contacts observed reveals a remarkable degree of versatility for the allosteric site, which is able to recognize specifically dissimilar compounds by employing the same residues.

Inhibitor Site

The inhibitor or caffeine (**13**) binding site binds flavopiridol (**14**) [35] (analogue complex shown in Fig. (**4**)) with a K_i of 1.16 μM for RMGPb inhibition [14]. Caffeine was found to bind with K_i's of 0.1 mM [36] and 0.08 mM [37] for RMGPa and RMGPb, respectively. The site is located on the surface of the enzyme at the entrance to the catalytic site (approximately 12 Å from it). In the T state, the phenyl ring of Phe285 (part of the 280s loop) is stacked close to that of Tyr613 and these two aromatic residues form the core of the inhibitor site. Inhibitor site GPIs work by stabilizing the T-state of the enzyme and blocking access of the glycogen substrate to the catalytic site. Binding at this site shows great diversity. Purines (e.g. adenine and caffeine), nucleosides (e.g. adenosine and inosine), nucleotides (e.g. AMP, IMP and ATP), NADH and certain related heterocyclic compounds such as FMN (flavin mono-nucleotide), FAD (flavin-adenine dinucleotide), and riboflavin have been shown to bind at this site in muscle GPb and GPa, but liver GPa shows a more stringent selectivity for inhibitors [8]. The interactions at this site are mainly hydrophobic with good inhibitor site GPIs having aromatic rings which can (π-π) stack between the side chains of Tyr613 and Phe285 forming sandwich type complexes; the type of inhibitors studied can be sourced in recent reviews [14, 15]. Inhibition at the inhibitor site is generally synergistic with glucose.

New Allosteric Site

The new allosteric or dimer interface (indole) binding site binds compound CP320626 (**15**) (PDB codes 1C50 [38]; 1H5U [39]; 1LWO [40]) and is located inside the central cavity formed on association of the two GP monomer

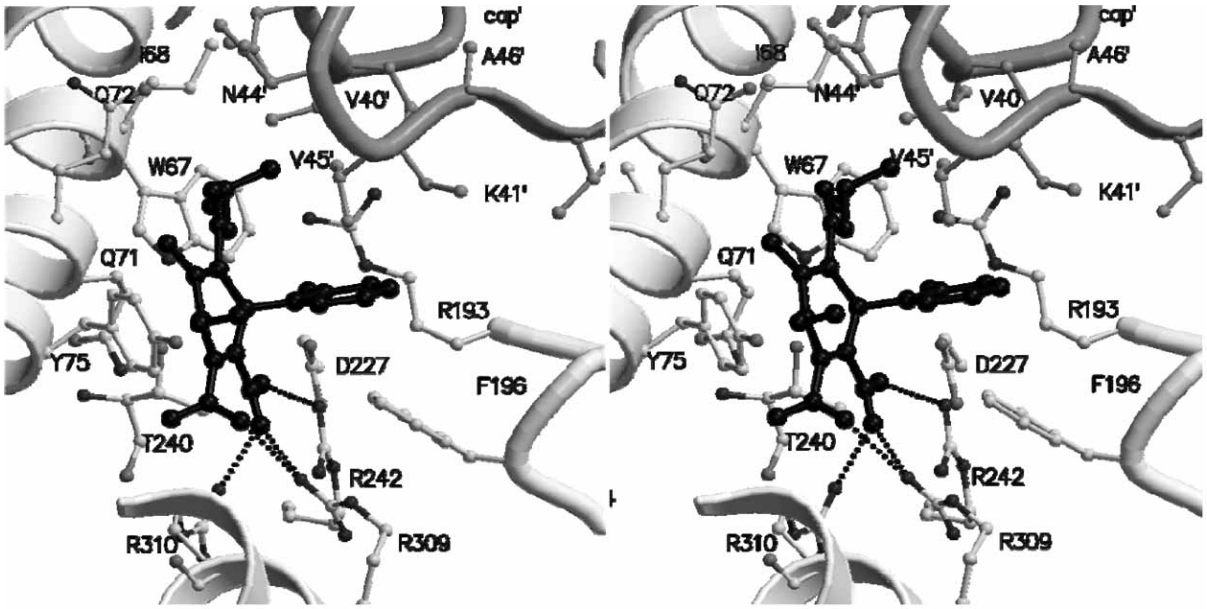

Fig. (3). The Bayer compound W1807 (**7**) bound at the allosteric site (PDB code 3AMV). The carboxylate oxygens of W1807 exploit the allosteric effector phosphate-recognition subsite which is composed of three arginine residues: Arg242, Arg309 and Arg310. The chlorine atom of the chlorophenyl group is buried in a pocket where it makes several van der Waals interactions to Arg193 and to Asp227. The chlorine appears to assist binding by filling this pocket on the protein surface. The chlorophenyl group is situated between the aromatic sidechain of Phe196 and the sidechain of Val45' with the two phenyl rings inclined approximately 40°. Several contacts are made from all atoms of the chlorophenyl ring to the edge of Phe196 (CE1 and CZ atoms), representing interactions from the δ^- π electron cloud of the chlorophenyl ring to the δ^+ hydrogen atoms on the Phe196. The ethyl group of W1807 (C1H and C1M) stacks against Tyr75 making some seven van der Waals contacts. The isopropyl group (C2H, C2M and C3M) contacts Trp67, Ile68 and the aliphatic part of Arg193. The high affinity of W1807 for GPb appears to arise from numerous non-polar interactions made between the ligand and the enzyme, especially those between CH groups and π electron orbitals of aromatic rings.

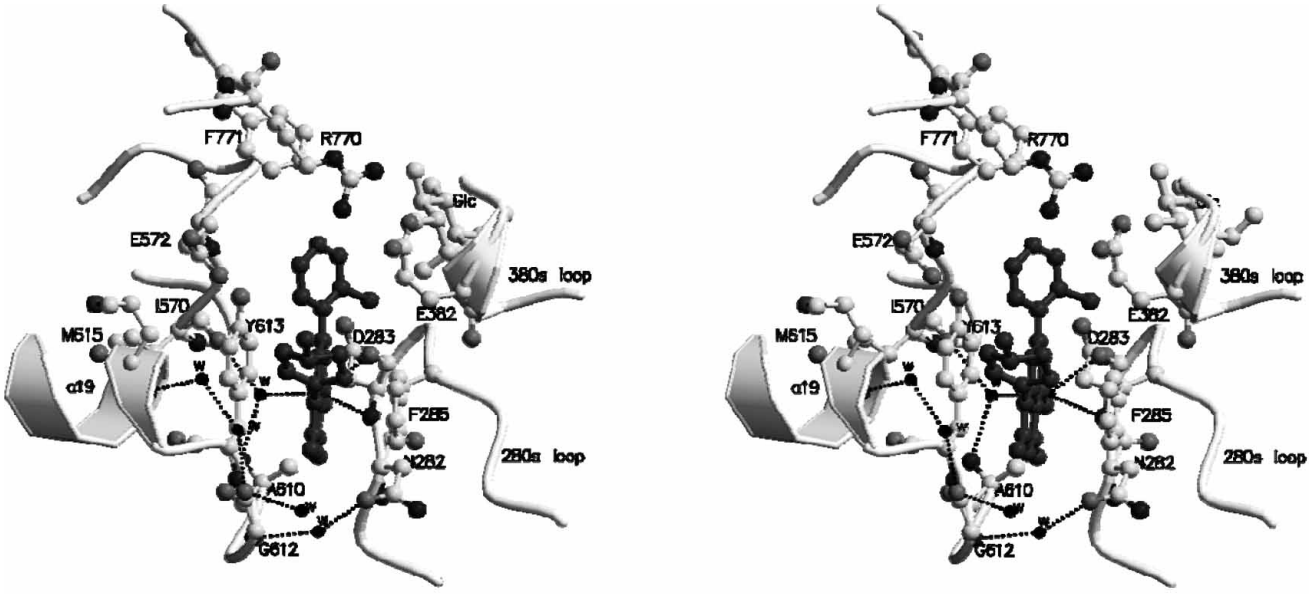

Fig. (4). Binding of a flavopiridol analogue at the inhibitor site [14]. The hydrogen bonding patterns between the ligand, protein residues and water molecules (shown as black spheres) are shown as dotted lines. The location of the catalytic site is indicated by the glucose (Glc) molecule. Although the hydrophobic sandwich stacking interactions of the molecule between residue Phe285 from 280s loop and Tyr613 from α19 helix (residues 613-631) forms the core of the receptor-ligand contacts, there are also a number of water-mediated hydrogen bonding interactions contributing to the GPI binding affinity. The affinities are higher in the presence of high glucose concentrations [14].

subunits (dimer interface). The binding of CP320626 from PDB code 1C50 to MGPb is shown in Fig. (**5**), highlighting the important residues. The central cavity is located about 15 Å from the allosteric site, 33 Å from the catalytic site and 37 Å from the inhibitor site. Inhibitors binding at this site stabilize the T-state conformation of the enzyme and hence inhibit GPb by locking the enzyme in an inactive state. The site, being solvent exposed, has a number of waters bridging receptor-ligand contacts. The structure of the GPb-CP320626 complex [38, 39] revealed specific chacteristics of this site. Inhibitor binding occurs with only small distortions of the structure, and with the displacement of nine water molecules. The increase in entropy from the release of these waters, together with the van der Waals, CH/π, halogen/polar, and the specific polar/polar interactions appear to be the major source of binding energy that support inhibitor binding. Although solvent exposed, hydrophobic pockets such as those formed by lipophilic side chains of amino acids including Leu63, Val64 and Trp67 can contribute to binding [41]. Hydrophilic and hydrophobic interactions stabilize the less active T state of the enzyme, however, one computational study of indole-2-carboxamide inhibitors estimated that the hydrophobic contribution to binding was close to 95% (*vide infra*, Section IV) [42].

Glycogen Storage Site

The glycogen storage site is on the surface of the molecule approximately 30 Å from the catalytic site, and 40 Å and 50 Å from the allosteric and new allosteric site, respectively. This binding site of GP has received little attention as a possible target in modifying activity of GP and there are no reported computational studies. However, binding of α-, β-, and γ-cyclodextrins (CD, cyclooligosaccharides of glycosidically α-1,4-linked 6, 7, or 8 D-glucopyranosyl units, respectively) have been studied kinetically and by protein crystallography with mM inhibition of RMGPb obtained [43].

Predicting a GPI Binding Site

X-ray structure determination of inhibitor bound GP complexes is very demanding, while competitive binding studies may not be suitable to identify the binding sites for some GPIs [44, 45]. Modeling calculations, therefore, provide an alternative but it is important sometimes to be cautious with respect to the predicted mode and action of new GPIs. In one study, docking lead the authors to suggest that the triterpene class of GPIs may bind at the inhibitor site [46], however, subsequent protein crystallography of the RMGPb–maslinic (**9**) (PDB ID: 2QN2) and RMGPb-asiatic (**10**) (PDB ID: 2QN1) complexes revealed the inhibitors bind at the AMP allosteric site [27]. On the other hand, using the 3D similarity/ superposition tool SQ [47], the binding site of the phenyl diacid compound **16** was predicted as the allosteric site [45] and subsequently confirmed by crystallography [48]. Meanwhile, studies of benzamide derivatives such as **17** (IC_{50} of 2.68 μM for RMGPa inhibition) suggested based on the mapping (using Catalyst 4.10 [49]) between pharmacophores for the different GP binding sites and conformers of the benzamide derivatives, that the inhibitors 'likely' bind at the new allosteric site [44]. The pharmacophore models for the four different binding sites (catalytic, inhibitor, allosteric and new allosteric) were created using LigandScout [50] and several protein-ligand PDB complexes. Receptor-ligand (complex) structure-based pharmacophores should be more reliable compared to those from 3D similarity. Glide-XP docking calculations have also recently been used to predict the binding site (allosteric site) of a se-

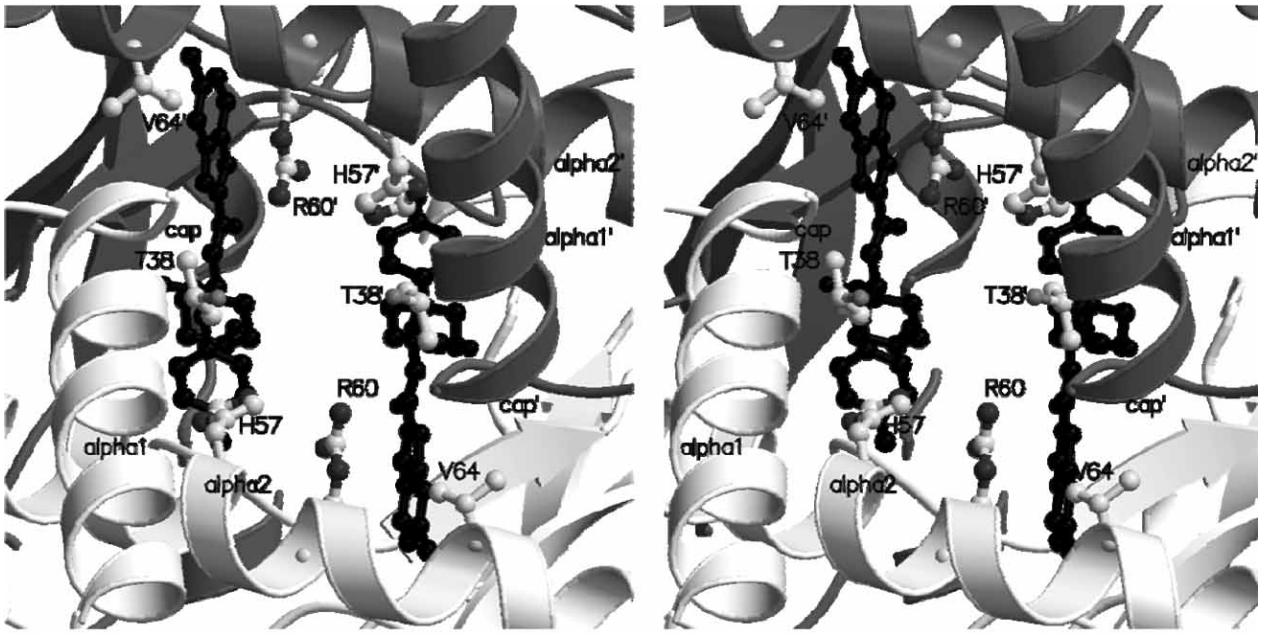

Fig. (5). The binding of CP320626 (**15**) at the new allosteric site. The site is formed when the two subunits (related by a crystallographic 2-fold symmetry axis) of the functionally active dimer associate. The site encompasses a solvent filled cavity surrounded on each side by residues from the N-terminal domains of both subunits. The cavity is about 30 Å long and the radius varies from a maximum of ~8 Å to a minimum of ~4 Å and occupies a volume of about 1300 $Å^3$ in the T-state GPb. The cavity is closed at one end by residues from the cap and a2 helices (Arg33, His34, Arg60 and Asp61 and their symmetry-related residues) and at the other end by the tower helices (residues Asn270, Glu273, Ser276 and their symmetry-related residues). In the 2.0 Å resolution 100K native T-state GPb structure (PDB code 2GPN), the cavity contains 60 located water molecules (30 waters and their symmetry-related equivalents). These waters have a few contacts with the protein and only 4 out of the 30 make more than one hydrogen bond to protein atoms.

ries of glucoconjugates of oleanic acid GPIs [51] (*vide infra*, Section IV), with experimental validation awaited.

In some instances GPIs may bind at two different binding sites; for example, indirubin-3'-aminooxy-acetate (E243 (**18**)) is a low μM range GP inhibitor and occupies the inhibitor site, but also binds two molecules at/near the allosteric site [52]. One E243 molecule binds at the allosteric site, while the second is bound at a subsite in the vicinity of the allosteric site. FR258900 (**19**) inhibits HLGPa with an IC_{50} value of 2.5 μM [53]. The crystal structure of the RMGPb-**19** complex was determined and revealed binding at the AMP allosteric site (K_i = 0.46μM for RMGPb inhibition) although **19** has no structural similarity to either of the natural allosteric regulators, activator AMP and inhibitor Glc-6-P [54]. In the case of the new allosteric site, it is expected that two GPI molecules bind together and hence interact not only with GP, but with each other to varying degrees. Birch and co-workers [55] revealed by crystallography (PDB IDs: 2IEG and 2IEI) that two inhibitor molecules of **20a** (GPa IC_{50} = 135 nM) and **20b** (GPa IC_{50} = 121 nM) bind at the dimer interface (new allosteric) site; the two ligands of **20a** adopt different orientations and in the case of **20b** there are hydrogen bond contacts between the two ligands, suggestive of cooperativity. Even for glucose analogue inhibitors binding at the catalytic site, it is possible that the GPIs may bind at a second site. For example, the benzoyl-urea derivative **6** (R = phenyl) also binds at the new allosteric site [20], while the glucopyranosylidene-spiro-isoxaxoline **4** (R = phenyl, X = NO_2) binds at the inhibitor site [18]. However, in both cases the binding at the second site is significantly weaker.

The latter examples are an indication of the potential difficulties encountered when predicting both GPI binding sites and the receptor-ligands interactions. There are also a number of GPIs with un-determined binding sites [14].

Choosing a GP Receptor Model

HLGPa is the more important target enzyme in terms of treatment of type 2 diabetes because of its direct influence on blood sugar levels. The HLGPa polypeptide chain is 846 residues long, compared with 841 and 842 residues for human muscle and rabbit muscle GPb, respectively. The muscle and liver enzymes are 79% identical with 100% identity at the glucose binding site (catalytic site), but the two isoenzymes differ in allosteric properties [56-58]. The vast majority of allosteric site GPIs are studied targetting GPa for this reason. The new allosteric sites in RMGP and HLGP are highly conserved; the only difference that Ala192 in RMGP is a serine in the HLGP isoenzyme. Comparison of the crystal structures of T-state HLGPa in complex with CP403700 (**21**) (or CP526423) and 1-GlcNAc [59] with their respective complexes with RMGPa revealed that the structures superimpose well and that they closely resemble eachother in the vicinity of the new allosteric site [8].

The facilitation of the growth of muscle GPb crystals from rabbit has lead to the deposition of a large number (more than 120) of co-crystallized RMGPb-GPI complex

structures (GPIs bound at the different sites) to the RCSB Protein Data Bank. This rather large number of crystal structures facilitates the SBDD approach. There are also a number of inhibitor complexes co-crystallised with GPa. Examples would be: for the catalytic site, there is the RMGPa – α-D-glucose (**1**) complex (PDB code 2GPA [25]); for the allosteric site, the RMGPa-glucose-W1807 (**7**) [PDB code 3AMV [25]] and RMGPa-caffeine (**13**)-W1807(**7**) complexes (PDB code 1C8L [60]), the HLGPa – α-D-glucose – **8b** complex (PDB code 2ATI [26]) and the series of GlaxoSmithKline anthranilimide based GPIs complexed with HLGPa – caffeine (PDBs codes 3DD1, 3DDS, 3DDW [28]); for the inhibitor site the caffeine (**13**) complexes just mentioned (PDB codes 1C8L [60] and 3DD1, 3DDS, 3DDW [28]) and the crystal structures of uric acid, caffeine and riboflavin in complex with HLGPa [61]; and for the new allosteric site, HLGPa with bound **22** and α-D-glucose (PDB code 2ZB2 [41]) , CP30626 (**15**) and CP403700 (**21**) with RMGPa – α-D-glucose and HLGPa – 1-GlcNAc, respectively (PDB codes 1LWO [40] and 1EXV [59], respectively).

In choosing a model PDB complex for calculations, the choice is influenced by such factors as those outlined above; the binding site(s) of the co-crystallized ligand(s); and the similarity of the co-crystallized ligand to new inhibitors being modeled. There are some differences in inhibition constants of GPIs for the different GP isoforms, but not significant differences [14].

SECTION III: COMPUTATIONAL METHODS *VERSUS* EXPENSE

Molecular Dynamics Free Energy (MDFE) calculations [62] in the form of free energy perturbation (FEP) MD simulations modelled accurately and explained the observed binding affinity differences [63] for a set of closely related glucopyranosylidene-spiro-hydantoin derivatives (**23**) binding at the GPb catalytic site. MDFE calculations represent the entire, or part of the biomolecular system and surrounding solvent in atomic detail, and provide the most accurate computational method for the evaluation of relative binding affinities of different ligands to a protein [64]. Accuracy of predictions is the holy grail in the design of new GPIs, but MDFE calculations are highly expensive and only viable for comparing potencies of no more than a few similar type GPI derivatives.

Whereas virtual screening has mainly been used in the "lead identification/discovery" [65] (a lead generally considered to bind on the (low) μM range), some docking methods can now also be used to improve potency in the "lead optimization" phase [66]. Very recently, Glide [67-69] docking calculations in extra-precision (XP) mode and in quantum-mechanics polarised ligand docking (QPLD) [67] were able to correctly rank the potencies of a set of glucose-based spiro-isoazolines (**4**) over a very short pK_i (2.2 log units) range [18]. In the QPLD calculations, the top-ranked ligand poses from initial Glide-XP calculations were reassigned ligand atomic partial charges by fitting to electrostatic potentials (ESPs) generated from single point energy (SPE) calculations on the ligand poses, either in the free state (no receptor) using QM or in the 'field' of the receptor using QM/MM. The ligands with the new partial charges were then redocked using Glide-XP. QPLD with the ligand charges calculated in the "field" of the receptor accounting for receptor-ligand charge polarization effects yielded the best results with a correlation (R^2) of 0.958 between docking GlideScores and experimental binding free energies (BFEs). Although the set of ligands studied was small (five GPIs) and contained similar type derivatives, the relative binding affinities of the set was reproduced with good accuracy and considerable less computational effort compared to full-scale MDFE simulations. It should be noted, however, that the accuracy of Glide and QPLD for ranking larger and more diverse sets of catalytic site GPIs has yet to be determined, especially if they induce varying conformational shifts in the vicinity of the site (e.g. 280s loop).

Docking algorithms are in continuous development and there are many articles reviewing their status, performance and future challenges [70-73]. Among the most popular docking programs are Glide [67-69], FlexX [74, 75], GOLD [76, 77], AutoDock [78-80] and DOCK [81]. One of the limitations of standard docking programs is the rigid receptor approximation used, and while receptor flexibility in docking calculations remains a challenge [82], a number of current docking algorithms now allow for at least some receptor flexibility in calculations (e.g. FlexX [75], GOLD [76], AutoDock [80]). The induced-fit docking (IFD) algorithm of Schrödinger [67, 83] allows one to refine receptor residues (using the program Prime [67]) surrounding an initial set of Glide docked ligand poses before redocking of ligands to the new receptor conformations. While this should in theory lead to more accurate geometries, the effect on the ranking of GPI potencies is uncertain, as is alternatively rescoring docking poses using, for example, the MM-GBSA (or MM-PBSA) methods which include receptor flexibility and implicit solvation effects [84-86]. The quality of results is quite possibly dependent on the GP binding site and its characteristics. In this regard, it has also been reported that energy minimization of docked poses can significantly improve ranking/enrichments in systems with sterically demanding binding sites [72], while Huang and co-workers have presented a very good overview of the use of different MM methods for ranking ligand binding affinities [87]. Meanwhile, the linear interaction energy (LIE) or linear response methods (LRM) for binding affinity predictions are "semi-empirical" approaches [88-90] retaining some of the theoretical aspects of FEP but including parameters derived from experimental data, hence are computationally faster but have less accuracy than FEP. Their application to GPI binding studies in the future would be interesting.

Computationally expensive QM and hybrid QM/MM calculations are becoming increasingly more important in SBDD applications, fueled by greater computational power and the development of more efficient algorithms for calculating wavefunctions of macromolecular systems [91, 92]. Important properties such as ESP maps for characterizing binding sites, protonation states (both ligand and residue), and polarization and charge transfer effects can be calculated. QM/MM type docking with QPLD was successfully applied to study binding of the spiro-isoazolines derivatives (**4**) to GP as outlined above [18], and QM-derived charges have also been shown to more accurately model binding in

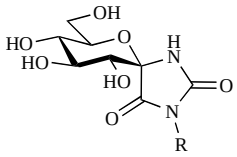

R	Ki (μM;RMGPb)[62,63]
H	3.1
Me	1200
NH_2	146

23
glucopyranosylidene-spiro-hydantoins

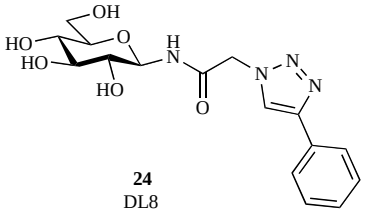

24
DL8
Ki = 0.18 mM (RMGPb) [117]

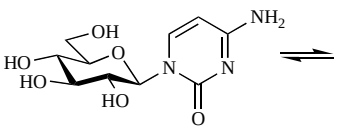

25a

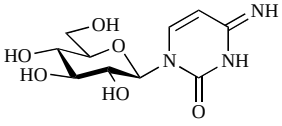

25b

25
β-D-glucopyranosyl pyrimidine
Ki = 7.7 μM (RMGPb) [23]

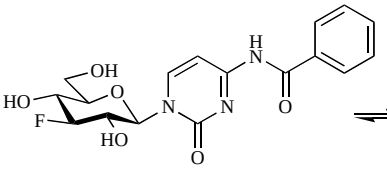

26a

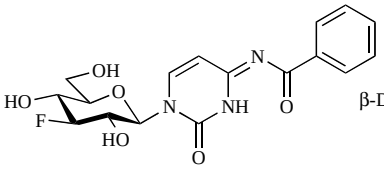

26b

26
(F-substituted)
β-D-glucopyranosyl pyrimidine
Ki = 46 μM (RMGPb) [22]

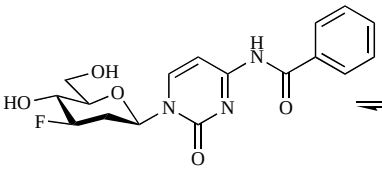

27a

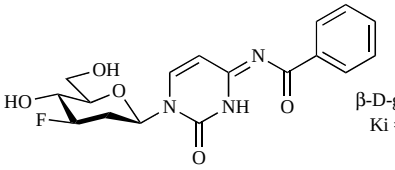

27b

27
(F-substituted)
β-D-glucopyranosyl pyrimidine
Ki = 6.55 mM (RMGPb) [22]

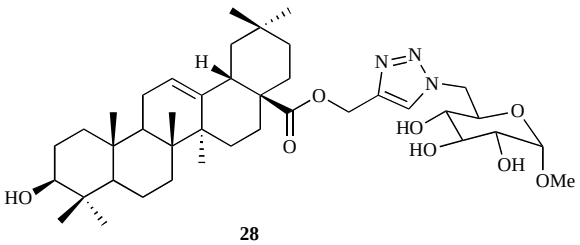

28
glucoconjugate of oleanic acid
IC_{50} = 1.14 μM (RMGPa) [51]

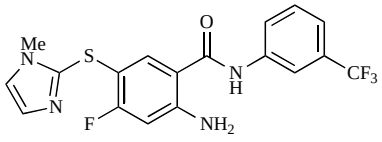

29
benzamide derivative
IC_{50} = 8.96 μM (HLGP) [141]

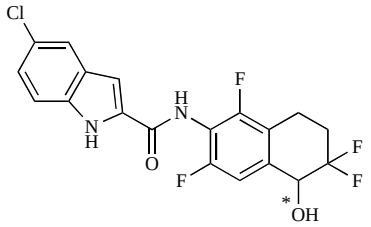

30eα(*R enantiomer); IC50 = 20 nM (HLGPa) [149]
30eβ (*S enantiomer); IC50 = 160 nM (HLGPa) [149]
Astellas Pharma
(N-bicyclo-5-chloro-1H-indole-2-carboxamide derivative)

other protein-ligand complexes [93, 94]. The ZINC database of commercially available drug-like molecules has been prepared with (semiempirical) QM charges and desolvation penalties [95]. QM/MM methods are now beginning to be used to help predict ligand binding affinities [96-99], and this may have applications in ranking GPIs binding at, for example, the inhibitor site where standard docking methods may fail (*vide infra*, Section IV). Already QM/MM has been applied to distinguish favored tautomeric forms of ligands binding at the GP catalytic site [22]. High level QM calculations also allow accurate enumeration of important unbound ligand properties, such as the relative energies of tautomeric forms of inhibitors that have the potential to bind to GP [22, 23]. Accurate pKa calculations of ligand ionization states are also now possible [23], using programs such as the Jaguar QM program with empirical corrections [67].

Computationally inexpensive QSAR methods have been widely used to model GPIs, where the QSAR models provide a mathematical relationship between the biological activity of a molecular system and its geometric and chemical characteristics. Widely use three dimensional (3D)-QSAR methods such as CoMFA [100] have been used to model ligand activity, as well as the more accurate receptor dependent (RD-)4D-QSAR method [21], which incorporates receptor effects into the QSAR models. Much of the QSAR work we have reviewed previously [14] but will be recapped in part together with the more recent work (*vide infra*). Examples of the use of pharmacophore modeling in GPI studies have already been given in Section II. Using this method, the inhibitor pharmacophore represents the ensemble of steric and electronic features necessary to optimize inhibitor-receptor interactions [101]. General features such as hydrogen bond donors, hydrogen bond acceptors, + and – charged groups, and hydrophobic regions are used, with the other key component the incorporation of the three dimensional nature of interactions into the (3D-)pharmacophore. Some pharmacophore methods use 3D-QSAR to refine their models or the two techniques are closely integrated [101]. Using an ensemble of methods with different degrees of computational expense/accuracy can also be considered. Following an initial comparison of binding affinity prediction methods for a set of 30 catalytic site GPIs [102], So and Karplus [103] used a multiple screening/layer approach to designing GPIs with the accuracy of each method (but also computational cost involved) increasing at each stage in the process. A preliminary filter using LUDI's [104-106] empirical scoring function was followed by a consensus 'activity prediction' stage using five QSAR based predictors (HQSAR [107], C2GNN [108, 109], CoMFA [100], SMGNN [110, 111], RSM [112, 113]). The final 'validation layer' (a structure-based prediction SBEP stage [102]) involved predictions based on an atomic forcefield and electrostatic calculations for the protein-ligand complexes.

To summarize, MDFE methods (FEP or thermodynamic integration) remain the most accurate for calculating (relative) binding affinities of similar GPIs [114]. Other methods described such as docking and QSAR are less accurate but have been efficiently applied to GPI studies. They can be used to quickly screen large sets of ligands compared to days to weeks (depending on computational resources/system setups) for a select few similar ligand derivatives using MDFE. However, should the synthetic route to a predicted inhibitor be very demanding [14], MDFE calculations may still be worthwhile to validate and strengthen predictions from lower level calculations. With computational capabilities constantly improving, and more efficient MDFE algorithms being developed such as the FEP/MD algorithms employed by the new Desmond program [115, 116], these calculations are becoming more accessible than in previous years.

SECTION IV: APPLICATION OF MODELING METHODS TO DIFFERENT GP BINDING SITES

Analysis of previous work can lead to vital clues in designing new modeling experiments. In this section a recap of the previously reported computational work [14] is integrated together with the newer work, so as to highlight the benefits of application of modeling methods to GPI design, often most profitable in combination with experiment.

Catalytic Site

As already mentioned, MDFE simulations [62] were used to calculate the relative binding affinities for GP of three glucopyranosylidene-spiro-hydantoin derivatives (**23**) in good agreement with experiment. Of further interest here is that a comparison of the interaction energies between a set of ligands and their surrounding groups in X-ray structures is often used in the interpretation of binding free energy differences and in guiding the design of new ligands. However, for the systems in this work such an approach failed to estimate the order of relative binding strengths. In contrast, a free-energy decomposition analysis showed that the replacement of a hydrogen by a methyl- or amino group reduced the binding affinity, due to steric interference with proximal protein groups and water molecules. The computed binding free energies were sensitive to the preference of a specific water molecule for two well-defined positions in the catalytic site.

The performance of Glide 4.0 [67-69] and GOLD 3.1.1 [76, 77] programs have been compared for modeling features of the binding of glucose analogue N-(β-D-glucopyranosyl)-(4-phenyl-1,2,3-triazol-1-yl) acetamide (DL8 (**24**)) at the catalytic site [117]. One of the attributes of GOLD docking is that it includes some receptor flexibility by allowing torsion angles of hydroxyl group residues (Ser, Thr and Tyr) and Lys NH_3^+ groups to be flexible so as to optimize hydrogen bonds; also, orientations of retained crystallographic waters can be sampled in the binding site and waters toggled on/off if obstructing ligand binding poses/conformations. Glide, meanwhile, uses a crude but effective explicit water model for modeling solvation effects with the pseudo-explicit water molecules placed after the initial docking. Both docking programs were able to very accurately redock **24** to its native protein structure receptor conformation (PDB code 2PYI), with the retention of the crystallographic waters not important. However, MD simulations for the binding of **24** with a flexible GP catalytic site, crystallographic waters deleted and the Generalized Born/Surface Area (GB/SA) [118] continuum model to describe bulk solvation effects lead to different binding modes compared to that seen in the crystal structure. It was necessary to retain the ordered crys-

tallographic cavity waters to model local solvation (miscro-solvation) effects in combination with the GB/SA continuum model for bulk solvation effects to obtain the correct binding geometry.

The accuracy of QPLD for ranking the catalytic site GPI set **4** has already been discussed [18]. Further, in the same work it was shown that applying docking constraints on the well-defined positions of the glucose moeities of the ligands improved results with respect to reproducing crystallographic ligand binding conformations and ranking of the binding affinities.

A very recent study [23] of β-D-glucopyranosyl pyrimidine derivatives revealed the importance of consideration of tautomeric forms of the ligands in the GPb binding studies; in the case of **25** (K_i of 7.7 μM for GPb inhibition), for example, two competitive binding (tautomeric) forms **25a** and **25b** are revealed using Glide 5.0 [67-69] (and QPLD) [67] docking calculations. Jaguar 7.5 [67] pKa calculations also revealed the potential of some inhibitors to bind in different ionization states. QM calculations were performed to identify the low energy tautomers of the ligands.

Catalytic site GPI design has focussed on glucose analogues (**3**) with α and β substitutions at the C1 position. In a follow-up study [22] of the binding features for another set of β-D-glucopyranosyl pyrimidine derivatives but with a flourine instead of a hydroxyl at the 3' position of the glucose moeity, Glide 5.0 [67-69] docking and QSite [67] QM/MM calculations also revealed the potential of the GPIs to bind in different tautomeric forms. Preferred binding of compound **26** through **26b** and **27** through **27a** was consistent with the Asp283 side chain carboxylate pointing towards and away from the ligands in the GPb-**26** and GPb-**27** crystal structures, respectively. The best inhibitor of the set (**26**) had a K_i of 46 μM for GPb inhibition, with the -F substitution not improving potencies over the native glucose -OH. Using further Glide and QPLD [67] calculations, a series of other substitutions at the 3' equatorial position were explored, but none of the substitutions were predicted to outperform –OH which acts as both a hydrogen bond donor and acceptor at this position.

In these studies for the binding of ligands in different tautomeric forms at the GP catalytic site [22, 23], results were influenced by the (rigid) receptor conformation used, the tautomers having different hydrogen bond donor/acceptor structural properties due to the local hydrogen migration. The importance of consideration of ligand tautomerism in computer-aided drug design has been highlighted before but this area had not yet received adequate attention [119-123].

Meanwhile, a number of 3D- and 4D-QSAR models [21, 24, 124-127] have been applied to model binding of sets of catalytic site inhibitors, reported in our previous review [14]. It should be reiterated that the merits of consideration of receptor-ligand induced fit effects involving catalytic site residue conformational changes have been highlighted [21, 24]. A new method called receptor dependent (RD-)4D-QSAR was developed and found to be more effective than receptor independent (RI-)4D-QSAR [21]. Although both methods gave similar statistics for the training set of 47 α and β substituted D-glucose ligands used to build the models (r^2 = 0.85; q^2 = 0.82 for both methods), when applied to the test set of 8 supplementary inhibitors assembled from reference [128], the RD-4D-QSAR approach clearly outperformed RI-4D-QSAR for the inhibitors with structural characteristics deviating from those included in the training set. Information about the receptor geometry embedded in the QSAR provides insight into the conformational changes in the receptor due to a particular bound ligand. Some of the main ligand induced receptor conformation changes involved were: two possible conformations of Asn284 (acting as hydrogen bond donor/acceptor); reorientation of phosphate group of PLP depending on glucose inhibitor β-substituents (**3**); reorientations of backbone carbonyl of His377 [21]. In a follow-up study, realignment and conformations of residues in the Ala673-Thr676 sequence, Leu136 and residues of the 280s and 380s loops in the RD-4D-QSAR models was also highlighted [24].

A new RI-4D-QSAR approach called (Laboratório de Quimiometria Teórica e Aplicada) LQTA-QSAR has recently been presented [129] and was applied to the same set of 47 catalytic site GPIs used in previous studies [21, 125, 127]. Generating a conformational ensemble profile (CEP) and interaction energies as descriptors for each inhibitor from GROMACS [130] MD simulations of the unbound ligands, the 3D descriptors for the LQTA-QSAR model were calculated in a manner which then incorporates the main features of both CoMFA [100] and 4D-QSAR [131]. A model with statistics r^2 = 0.81 and q^2 = 0.72 for 12 selected variables was obtained. LQTA-QSAR can be found on the internet at http://lqta.iqm.unicamp.br

Verma and colleagues [132] developed a new 3D-QSAR approach called local indices for similarity analysis (LISA) and validated it on a set of previously assembled [133] 66 glucose analogue GPIs. LISA estimates molecular similarity at the local level (local similarity index (LSI)), allowing to interpret the resulting models based on structural features. The LISA results were compared with CoMFA and CoMSIA models calculated with Sybyl 7.1 and gave comparable results/statistics. The output from LISA can be graphically displayed providing suggestions on structure modifications to improve inhibitor binding affinites. For calculating the local similarity at a certain point on the grid surrounding a molecule, the potential (e.g. electrostatic, steric, lipophilic, etc.) is compared to that of a reference molecule; the choice of reference is important, with the most active molecule recommended.

To summarize, despite the flexibility of the 280s loop, rigid receptor docking programs (flexible ligand) have been successfully applied to model binding of GPIs at the catalytic site. This may, however, be dependent on the degree of the shift in the 280s loop and the variance in ligand induced conformational changes involved. This viewpoint can be considered consistent with Hopfinger's findings using RD-4D-QSAR models [21, 24], as just described. Larger ligands may result in larger shifts, but similar ligands may result in similar shifts in which case success may be expected. For example, multiple protein structure (MPS) docking using Glide 4.5 [67-69] was used to investigate the receptor struc-

ture/conformation dependence on docking results for a set of seven *N*-acyl-*N*'-β-D-glucopyranosyl ureas ligands **(6)** with a common NHCONHCO linker but varying shifts in the 280s loop residues depending on R substituents [14, 20]. Receptors for docking were derived from the co-crystallized complexes and MPS native- and cross-docking calculations of the ligands to their own and the other receptor structures performed, respectively. For reproducing the experimental binding structures and relative potencies, the single rigid receptor approximation was still reasonably valid using receptors prepared from the co-crystallized complexes with the bulkier R substituents which opened up the cavity in regions complementary to binding of the other ligands. It should also be mentioned that retaining the ordered crystallographic water molecules common to all receptor-ligands complexes in the docking calculations helped to orientate the NHCONHCO moieties in their correct crystallographic positions.

Inhibitor Site

Inhibitor site GPIs form interactions which are mainly hydrophobic with ligands sandwiched between Phe285 and Tyr613 by π-stacking interactions. However, in addition to the π-stacking, inhibitors can form direct or water mediated hydrogen bonding interactions to residues in the vicinity of the inhibitor site (*c.f.* Fig. (**4**)). To our knowledge, there are to date no reported modeling studies for binding at this site. Docking and MM methods currently struggle to accurately describe and score interactions involving π-electrons. QSAR approaches may be most effective for modeling inhibitor sites GPIs, however, QM/MM methods are also an option with the stacking interactions described using QM methods. Calculation of the stacking energy is tedious requiring a combination of the most accurate QM procedures (CCSD(T)) and very large basis sets, ideally extrapolating to the complete basis set (CBS) limit. However, recently DFT functionals have been developed which can be applied to calculate stacking interactions at much less computational cost [134, 135].

Allosteric Site

Using an iterative approach to allosteric site GPI design, an acyl urea derivative **8c** with potent inhibition in both enzyme (HLGPa enzyme IC_{50} = 53 nM) and cell-based (rat hepatocytes IC_{50} = 380 nM) assays was obtained [26]. **8c** was tested in Wistar rats and significantly reduced glucagon-induced hyperlycemia. The acyl urea derivative **8a** was used as the initial lead, identified by focused screening of 60 compounds exhibiting pharmacophoric similarities to known GP inhibitors. Structural optimizations were guided by 3D pharmacophore modeling using Catalyst 4.7 (HypoGen module) [49] and by 3D structural information from select determined RMGPb-inhibitor crystal complexes (PDB codes 1WUT (lead **8a** [136]) and 2ATI (**8b** [26])). The 3D pharmacophore hypotheses were key to the choice and design of experiment, however, the limitations of a 3D pharmacophore model were overcome by derivation of supplementary 3D-QSAR (CoMFA with Sybyl 6.9) models to more accurately account for electrostatic and hydrophobic interactions in quantitative affinity predictions (r^2 = 0.92; q^2 = 0.66); 3D-QSAR in combination with the 3D pharmacophore, therefore, were used to guide the chemical optimizations.

Li and co-workers [137] have also modeled using QSAR the affinities of the same series of acyl ureas [26]. Effective QSAR models using structural descriptors encoding constitutional, topological, geometrical, electrostatic and quantum chemical features were constructed using multiple linear regression (MLR) (r(training set) = 0.897; r(test set) = 0.88) and least squares support vector machines (LS-SVMs) (r(training set) = 0.957; r(test set) = 0.899).

A series of glucoconjugates of oleanic acid (OA) where OA and a glycoside are linked through either a triazole or ester linkage have been studied [51]. The most potent RMGPa inhibitor of this series **28** had an IC_{50} of 1.14 μM compared to an IC_{50} of 14 μM for the parent OA [27]. The possible binding site and binding modes of **28** were investigated using Glide-XP [67-69] docking calculations. Docking calculations to the allosteric, inhibitor, catalytic and dimer interface sites were performed. The receptor for docking was prepared using the GPb-asiatic acid crystal structure (PDB ID: 2QN1[27]) with the GPb dimer generated using symmetry operations. However, asiatic acid is bound at the allosteric site in the crystal, so that there may have been some bias in the rigid receptor docking calculations. **28** was proposed to bind at the allosteric site exclusively, with the OA moeity positioned similar to asiatic acid in the 2QN1 crytal structure.

ICM docking [138] of the phenyl diacid **16** as a lead compound (R = NO_2) to the AMP allosteric site followed by calculation of grid based hydrophobic/hydrophilic surfaces using the docking model revealed an unfilled hydrophobic region near the central phenyl ring A [45]; using this information a series of napthyl diacid analogues (different R groups, napthyl group replacing phenyl ring A) with stronger binding affinities was designed.

New Allosteric Site

For the new allosteric site, docking and 3D-QSAR calculations by different groups on a set of 25 indole-2-carboxamide inhibitors [139] have been performed [42, 140], as described before [14]. Docking calculations using AutoDock 3.0 [78, 79] were performed [42] using the receptor from the HLGPa – CP403700 (**21**) complex (PDB entry 1EXV [59]) followed by derivation of more predictive 3D-QSAR models using both CoMFA (r^2 = 0.996; q^2 = 0.697) and CoMSIA (r^2 = 0.965; q^2 = 0.622) methods from the alignment conformations of the docked ligands. However, it should be noted that good correlation (r^2 = 0.710) between the predicted ligand relative binding affinities (docking scores) and the experimental activities (-logIC_{50}) was also obtained directly using AutoDock 3.0; it was estimated that the average electrostatic contribution to ligand binding was just ~ 6.1%, consistent with mainly hydrophobic interactions of the site [59].

Following the work on benzamide derivatives such as **17** described above (Section II) [44], in a different approach to design of anti-diabetic drugs, dual-action hypoglycemic benzamide derivatives which can both inhibit GP and activate glucokinase (GS) were investigated [141]. GS is a cytoplasmic enzyme whose activation is expected to improve glycemic control by phosphorylating glucose in the liver promot-

ing glycogen synthesis; in the pancreatic β-cells this also triggers glucose-sensitive insulin release [142]. **29** inhibited HLGP with an IC_{50} of 8.96 μM and activated GK with an EC_{50} of 1.87 μM. Docking calculations were performed using Glide in XP mode [67-69] to both targets and binding interactions for the docked benzamide compounds at the GP new allosteric, dimer interface site were proposed.

SECTION V: DESIGNING INHIBITORS WITH DRUG-LIKE PROPERTIES

Inhibitor design efforts are mainly focused on modifying ligand structure so as to improve its potency. However, inadequate absorption, distribution, metabolism (ADME) and toxicity (Tox) properties (ADMET) cause approximately 50% of drug candidates to fail [143, 144]. It can be more efficient and cost effective therefore to monitor these properties at an earlier stage in the inhibitor/drug design process with ideally integration of experimental and *in silico* technologies proposed by some [145].

Recently, GlaxoSmithKline released a series of papers on the optimization of anthranilimide based GPIs which bind at the AMP site [28, 146-148]. The crystal structure of HLGPa with **11** was determined (PDB code 3DDS), and the culmination of SAR studies for optimization of both *in vitro* and *in vivo* properties was GPIs such as **12** with nM inhibition in both enzyme (GPa IC_{50} = 3 nM) and cell-based (IC_{50} = 145 nM) assays, and which was also able to "acutely" lower glucose levels in a diabetic mouse model (ob/ob). Interestingly, despite a set of GPIs having similar *in vitro* activities, **12** would have been predicted by SAR to be the most active; *in vivo* **12** was found to be significantly more active. Follow-up publications will profile the pharmacokinetic properties of the compounds.

Using CP-320626 (**15**) as a benchmark for further design, Astellas Pharma Inc. [149] explored N-bicyclo-5-chloro-1H-indole-2-carboxamide derivatives in the design of GPIs acting at the dimer interface site. Exploiting the SAR data from the derivatives, they designed optically active compound **30eα** (R enantiomer) which had an IC_{50} of 20 nM for HLGPa inhibition (the IC_{50} of the corresponding S enantiomer **30eβ** was 160 nM). **30eα** inhibited glucose output from hepatocytes (IC_{50} of 690 nM) and hypoglycemic activity in diabetic db/db mice. It also revealed impressive pharmacokinetics in male SD rats with high oral bioavailability (F = 100%) and a long half-life ($t_{1/2}$ = 12 h). With X having four fluorine atoms, the pharmacokinetic profile is consistent with fluorine assisting the drug metabolism properties [150]. A simple "docked" model based on the positions of **22** in complex with HLGPa molecules (PDB ID: 2ZB2) [41] was obtained.

Such thorough *in vivo*/pharmacokinetic (and even *in vitro* cell assay) analysis are beyond the resources of many working outside the pharmaceutical industry. The relatively few recent publications highlight this [28, 41, 55, 149, 151]. However, ADMET property predictions offers a viable alternative towards the goal of drug-like inhibitor design [152-154] and there are a number of free resources available to do so [155, 156]. A recent review highlights some of the available software for ligand toxicity predictions [157]. Modules such as QikProp [67] (ADME property predictions) from Schrödinger are also available through the drug discovery commercial sofware packages. Using such packages, fulfillment, or not, of simple rules such as Lipinski's 'rule of five' [158, 159] and Veber *et al.*'s [160] suggested properties for oral bioavailability can help monitor the drug-likeness of GPIs at an earlier stage in the drug design process.

Descriptors used to model pharmacokinetic properties are also involved in receptor-ligand binding properties. Therefore, for a set of 23 catalytic site GPIs, Zamora and co-workers [161] were able to obtain a statistically significant model for binding affinity prediction (r^2 = 0.94; q^2 = 0.89) by integrated use of the VolSurf 2.0 [162, 163] descriptors based on the GRID [164] interaction fields which allowed simulataneous modeling of both protein-ligand binding affinities and ligand pharmacokinetic properties. The method, however, is alignment independent and hence chemical modifications can not be suggested for inhibitor optimization as is possible with standard 3D-QSAR.

Solubility properties of GPIs can lead to failure of inhibitors at a very early stage in the development process. For example, a series of thiazolidine-2,4-diones attached to 2,3-dihydrobenzo[1,4]dioxin ring systems was prepared [165] but because of solubility problems only a few of the final series and the intermediates could be assayed with GP. Simple solubility (log P) calculations [166, 167] can help prevent these problems prior to undertaking the time-consuming experiments including the initial synthesis.

Finally, matched molecular pair analysis (MMPA) [168] can be used to integrate potency with physiochemical properties, with Birch and co-workers [169] demonstrating how MMPA can be used as a predictive tool of activity and physicoproperties of GPIs which are linked to specific structural changes. Using MMPA, the difference in a property can be predicted more accurately than the property itself, leading to an analogy to be drawn with the FEP method.

SECTION VI: CONCLUDING REMARKS

The role of computation in serious current-day SBDD is now well established, with the development of new algorithms and improvements in existing software creating even more powerful tools. Adequate modeling of, for example, receptor flexibility as highlighted in this paper remains an on-going challenge in SBDD, but its incorporation in docking is receiving much recent attention [82, 170-173] and has been already successfully included in RD-4D-QSAR models for binding of GP catalytic site inhibitors [21, 24]. The design of GPIs exploiting computational methods have mainly focused on analogues of glucose binding at the catalytic site, for which both docking and QSAR methods are proving very effective. Other GP binding sites have been less explored and predominantly studied using QSAR models, with the π-stacking effects seen at the allosteric and inhibitor site more difficult to accurately describe using standard docking programs.

Glide [67-69] (catalytic site [18, 20, 22, 23, 117], allosteric [51] and new allosteric site [141]), GOLD [76, 77] (catalytic site [117]), AutoDock [78-80] (new allosteric site [42, 44]), LUDI [104-106] (catalytic site [42, 102, 103]) and ICM [138](allosteric site [45]) docking programs have all

been applied in GPI binding studies. There are a number of insightful publications comparing the performance of different docking programs which may be of interest to the GP modeler (for references, see [174]). For example, despite GP not being included as a target in a detailed comparison of the performance of Glide [67-69], GOLD [76, 77] and ICM [138] docking programs for other target proteins [72], Glide was found to perform more consistently with respect to diversity of binding sites; the performance of GOLD and ICM was more binding site dependent and particularly poorer for hydrophobic binding sites. Meanwhile, ADMET property predictions have not yet become mainstream in modern day GPI design, which should be a consideration given their likelihood to lead to eventual drug candidate failure.

ACKNOWLEDGEMENTS

The authors would like to acknowledge financial support from the Commission of the European Communities – under the FP7 "SP4-Capacities Coordination and Support Action, Support Actions" EUROSTRUCT project (CSA-SA_FP7-REGPOT-2008-1 Grant Agreement No. 230146). Michalis Mamais and Christos Lamprakis are acknowledged for their contributions to the GP modeling work performed with the SBCG group at the NHRF; George Archontis for collaboration on some modeling work and for his constructive comments regarding this manuscript.

ABBREVIATIONS

GP	=	glycogen phosphorylase
GPI	=	glycogen phosphorylase inhibitor
RMGP	=	rabbit muscle glycogen phosphorylase
HLGP	=	human liver glycogen phosphorylase
PLP	=	pyridoxal-5'-phosphate
glucose	=	α-D-glucose
Glc-1-P	=	α-D-glucose 1-phosphate
Glc-6-P	=	α-D-glucose 6-phosphate
AMP	=	adenosine monophosphate
ATP	=	adenosine triphosphate
IMP	=	inosine monophosphate
UDP	=	uridine 5'-diphosphate
NADH	=	nicotinamide adenine dinucleotide
(Q)SAR	=	(quantatative) structure activity relationship
MM	=	molecular mechanics
QM	=	quantum mechanics
QM/MM	=	quantum mechanics/ molecular mechanics
DFT	=	density functional theory
MM-GBSA	=	molecular mechanics/ generalized Born surface area
MM-PBSA	=	molecular mechanics/ Poisson Boltzmann surface area
CoMFA	=	Comparative Molecular Field Analysis
CoMSIA	=	Comparative Molecular Similarity Indices Analysis
CCSD(T)	=	Coupled Cluster Single Double (perturbative Triple)

REFERENCES

[1] Gershell, L. Type 2 diabetes market. *Nat. Rev. Drug Discov.*, **2005**, *4*, 367-368.

[2] Murata, G. H.; Duckworth, W. C.; Hoffman, R. M.; Wendel, C. S.; Mohler, M. J.; Shah, J. H. Hypoglycemia in type 2 diabetes: a critical review. *Biomed. Pharmacother.*, **2004**, *58*, 551-559.

[3] Wagman, A. S.; Nuss, J. M. Current therapies and emerging targets for the treatment of diabetes. *Curr. Pharm. Des.*, **2001**, *7*, 417-450.

[4] Hellerstein, M. K.; Neese, R. A.; Linfoot, P.; Christiansen, M.; Turner, S.; Letscher, A. Hepatic gluconeogenic fluxes and glycogen turnover during fasting in humans. A stable isotope study. *J. Clin. Invest.*, **1997**, *100*, 1305-1319.

[5] Andersen, B.; Rassov, A.; Westergaard, N.; Lundgren, K. Inhibition of glycogenolysis in primary rat hepatocytes by 1, 4-dideoxy-1,4-imino-D-arabinitol. *Biochem. J.*, **1999**, *342*, 545-550.

[6] Baker, D. J.; Timmons, J. A.; Greenhaff, P. L. Glycogen phosphorylase inhibition in type 2 diabetes therapy: a systematic evaluation of metabolic and functional effects in rat skeletal muscle. *Diabetes*, **2005**, *54*, 2453-2459.

[7] Lukacs, C. M.; Oikonomakos, N. G.; Crowther, R. L.; Hong, L. N.; Kammlott, R. U.; Levin, W.; Li, S.; Liu, C. M.; Lucas-McGady, D.; Pietranico, S.; Reik, L. The crystal structure of human muscle glycogen phosphorylase a with bound glucose and AMP: an intermediate conformation with T-state and R-state features. *Proteins*, **2006**, *63*, 1123-1126.

[8] Oikonomakos, N. G. Glycogen phosphorylase as a molecular target for type 2 diabetes therapy. *Curr. Protein Pept. Sci.*, **2002**, *3*, 561-586.

[9] Treadway, J. L.; Mendys, P.; Hoover, D. J. Glycogen phosphorylase inhibitors for treatment of type 2 diabetes mellitus. *Expert Opin. Invest. Drugs*, **2001**, *10*, 439-454.

[10] Sprang, S. R.; Acharya, K. R.; Goldsmith, E. J.; Stuart, D. I.; Varvill, K.; Fletterick, R. J.; Madsen, N. B.; Johnson, L. N. Structural changes in glycogen phosphorylase induced by phosphorylation. *Nature*, **1988**, *336*, 215-221.

[11] Barford, D.; Johnson, L. N. The allosteric transition of glycogen phosphorylase. *Nature*, **1989**, *340*, 609-616.

[12] Barford, D.; Hu, S. H.; Johnson, L. N. Structural mechanism for glycogen phosphorylase control by phosphorylation and AMP. *J. Mol. Biol.*, **1991**, *218*, 233-260.

[13] Sprang, S. R.; Withers, S. G.; Goldsmith, E. J.; Fletterick, R. J.; Madsen, N. B. Structural basis for the activation of glycogen phosphorylase b by adenosine monophosphate. *Science*, **1991**, *254*, 1367-1371.

[14] Somsak, L.; Czifrak, K.; Toth, M.; Bokor, E.; Chrysina, E. D.; Alexacou, K. M.; Hayes, J. M.; Tiraidis, C.; Lazoura, E.; Leonidas, D. D.; Zographos, S. E.; Oikonomakos, N. G. New inhibitors of glycogen phosphorylase as potential antidiabetic agents. *Curr. Med. Chem.*, **2008**, *15*, 2933-2983.

[15] Oikonomakos, N. G.; Somsak, L. Advances in glycogen phosphorylase inhibitor design. *Curr. Opin. Invest. Drugs*, **2008**, *9*, 379-395.

[16] Bharatam, P. V.; Patel, D. S.; Adane, L.; Mittal, A.; Sundriyal, S. Modeling and informatics in designing anti-diabetic agents. *Curr. Pharm. Des.*, **2007**, *13*, 3518-3530.

[17] Martin, J. L.; Veluraja, K.; Ross, K.; Johnson, L. N.; Fleet, G. W.; Ramsden, N. G.; Bruce, I.; Orchard, M. G.; Oikonomakos, N. G.; Papageorgiou, A. C.; Leonidas, D. D.; Tsitoura, H. S. Glucose analogue inhibitors of glycogen phosphorylase: the design of potential drugs for diabetes. *Biochemistry*, **1991**, *30*, 10101-10116.

[18] Benltifa, M.; Hayes, J. M.; Vidal, S.; Gueyrard, D.; Goekjian, P. G.; Praly, J. P.; Kizilis, G.; Tiraidis, C.; Alexacou, K. M.; Chrysina, E. D.; Zographos, S. E.; Leonidas, D. D.; Archontis, G.; Oikonomakos, N. G. Glucose-based spiro-isoxazolines: a new family of potent glycogen phosphorylase inhibitors. *Bioorg. Med. Chem.*, **2009**, *17*, 7368-7380.

[19] Watson, K. A.; Mitchell, E. P.; Johnson, L. N.; Cruciani, G.; Son, J. C.; Bichard, C. J.; Fleet, G. W.; Oikonomakos, N. G.; Kontou, M.; Zographos, S. E. Glucose analogue inhibitors of glycogen phosphorylase: from crystallographic analysis to drug prediction using GRID force-field and GOLPE variable selection. *Acta Crystallogr. D Biol. Crystallogr.*, **1995**, *51*, 458-472.

[20] Chrysina, E. D.; Nagy, V.; Felfoldi, N.; Telepo, K.; Praly, J. P.; Docsa, T.; Gergely, P.; Alexacou, K. M.; Hayes, J. M.; Leonidas, D. D.; Zographos, S. E.; Oikonomakos, N. G.; Somsak, L. *in preparation*.

[21] Pan, D. H.; Tseng, Y. F.; Hopfinger, A. J. Quantitative structure-based design: Formalism and application of receptor-dependent RD-4D-QSAR analysis to a set of glucose analogue inhibitors of glycogen phosphorylase. *J. Chem. Inf. Comput. Sci.*, **2003**, *43*, 1591-1607.

[22] Tsirkone, V. G.; Tsoukala, E.; Lamprakis, C.; Manta, S.; Hayes, J. M.; Skamnaki, V. T.; Drakou, C.; Zographos, S. E.; Komiotis, D.; Leonidas, D. D. 1-(3-Deoxy-3-fluoro-beta-D-glucopyranosyl) pyrimidine derivatives as inhibitors of glycogen phosphorylase b: Kinetic, crystallographic and modeling studies. *Bioorg. Med. Chem.*, **2010**, *18*, 3413-3425.

[23] Cismas, C.; Hayes, J. M.; Sovantzis, D.; Hadjiloi, T.; Mamais, M.; Lazoura, E.; Grammatopoulos, P.; Panagopoulos, D.; Zographos, S. E.; Leonidas, D. D.; Oikonomakos, N. G.; Gimisis, T.; Chrysina, E. D. *in preparation*.

[24] Pan, D. H.; Liu, J. Z.; Senese, C.; Hopfinger, A. J.; Tseng, Y. Characterization of a ligand-receptor binding event using receptor-dependent four-dimensional quantitative structure-activity relationship analysis. *J. Med. Chem.*, **2004**, *47*, 3075-3088.

[25] Oikonomakos, N. G.; Tsitsanou, K. E.; Zographos, S. E.; Skamnaki, V. T.; Goldmann, S.; Bischoff, H. Allosteric inhibition of glycogen phosphorylase a by the potential antidiabetic drug 3-isopropyl 4-(2-chlorophenyl)-1,4-dihydro-1-ethyl-2-methyl-pyridine-3,5,6-tricarbo xylate. *Protein Sci.*, **1999**, *8*, 1930-1945.

[26] Klabunde, T.; Wendt, K. U.; Kadereit, D.; Brachvogel, V.; Burger, H. J.; Herling, A. W.; Oikonomakos, N. G.; Kosmopoulou, M. N.; Schmoll, D.; Sarubbi, E.; von Roedern, E.; Schonafinger, K.; Defossa, E. Acyl ureas as human liver glycogen phosphorylase inhibitors for the treatment of type 2 diabetes. *J. Med. Chem.*, **2005**, *48*, 6178-6193.

[27] Wen, X.; Sun, H.; Liu, J.; Cheng, K.; Zhang, P.; Zhang, L.; Hao, J.; Ni, P.; Zographos, S. E.; Leonidas, D. D.; Alexacou, K. M.; Gimisis, T.; Hayes, J. M.; Oikonomakos, N. G. Naturally occurring pentacyclic triterpenes as inhibitors of glycogen phosphorylase: synthesis, structure-activity relationships, and X-ray crystallographic studies. *J. Med. Chem.*, **2008**, *51*, 3540-3554.

[28] Thomson, S. A.; Banker, P.; Bickett, D. M.; Boucheron, J. A.; Carter, H. L.; Clancy, D. C.; Cooper, J. P.; Dickerson, S. H.; Garrido, D. M.; Nolte, R. T.; Peat, A. J.; Sheckler, L. R.; Sparks, S. M.; Tavares, F. X.; Wang, L.; Wang, T. Y.; Weiel, J. E. Anthranilimide based glycogen phosphorylase inhibitors for the treatment of type 2 diabetes. Part 3: X-ray crystallographic characterization, core and urea optimization and *in vivo* efficacy. *Bioorg. Med. Chem. Lett.*, **2009**, *19*, 1177-1182.

[29] Monod, J.; Wyman, J.; Changeux, J. P. On the Nature of Allosteric Transitions: A Plausible Model. *J. Mol. Biol.*, **1965**, *12*, 88-118.

[30] Goldmann, S.; Ahr, H.-J.; Puls, W.; Bischoff, H.; Petzinna, D.; Schlossmann, K.; Bender, J. US Patent 4, 786, 641, Bayer AG (Leverkusen, Germany). 1988.

[31] Bergans, N.; Stalmans, W.; Goldmann, S.; Vanstapel, F. Molecular mode of inhibition of glycogenolysis in rat liver by the dihydropyridine derivative, BAY R3401: inhibition and inactivation of glycogen phosphorylase by an activated metabolite. *Diabetes*, **2000**, *49*, 1419-1426.

[32] Zographos, S. E.; Oikonomakos, N. G.; Tsitsanou, K. E.; Leonidas, D. D.; Chrysina, E. D.; Skamnaki, V. T.; Bischoff, H.; Goldmann, S.; Watson, K. A.; Johnson, L. N. The structure of glycogen phosphorylase b with an alkyldihydropyridine-dicarboxylic acid compound, a novel and potent inhibitor. *Structure*, **1997**, *5*, 1413-1425.

[33] Johnson, L. N.; Snape, P.; Martin, J. L.; Acharya, K. R.; Barford, D.; Oikonomakos, N. G. Crystallographic binding studies on the allosteric inhibitor glucose-6-phosphate to T state glycogen phosphorylase b. *J. Mol. Biol.*, **1993**, *232*, 253-267.

[34] Kristiansen, M.; Andersen, B.; Iversen, L. F.; Westergaard, N. Identification, synthesis, and characterization of new glycogen phosphorylase inhibitors binding to the allosteric AMP site. *J. Med. Chem.*, **2004**, *47*, 3537-3545.

[35] Oikonomakos, N. G.; Schnier, J. B.; Zographos, S. E.; Skamnaki, V. T.; Tsitsanou, K. E.; Johnson, L. N. Flavopiridol inhibits glycogen phosphorylase by binding at the inhibitor site. *J. Biol. Chem.*, **2000**, *275*, 34566-34573.

[36] Kasvinsky, P. J.; Madsen, N. B.; Sygusch, J.; Fletterick, R. J. Regulation of Glycogen Phosphorylase-a by Nucleotide Derivatives - Kinetic and X-Ray Crystallographic Studies. *J. Biol. Chem.*, **1978**, *253*, 3343-3351.

[37] Madsen, N. B.; Shechosky, S.; Fletterick, R. J. Site-Site Interactions in Glycogen Phosphorylase-B Probed by Ligands Specific for Each Site. *Biochemistry*, **1983**, *22*, 4460-4465.

[38] Oikonomakos, N. G.; Skamnaki, V. T.; Tsitsanou, K. E.; Gavalas, N. G.; Johnson, L. N. A new allosteric site in glycogen phosphorylase b as a target for drug interactions. *Structure*, **2000**, *8*, 575-84.

[39] Oikonomakos, N. G.; Zographos, S. E.; Skamnaki, V. T.; Archontis, G. The 1.76 A resolution crystal structure of glycogen phosphorylase B complexed with glucose, and CP320626, a potential antidiabetic drug. *Bioorg. Med. Chem.*, **2002**, *10*, 1313-1319.

[40] Oikonomakos, N. G.; Chrysina, E. D.; Kosmopoulou, M. N.; Leonidas, D. D. Crystal structure of rabbit muscle glycogen phosphorylase a in complex with a potential hypoglycaemic drug at 2.0 A resolution. *Biochim. Biophys. Acta*, **2003**, *1647*, 325-32.

[41] Onda, K.; Suzuki, T.; Shiraki, R.; Yonetoku, Y.; Negoro, K.; Momose, K.; Katayama, N.; Orita, M.; Yamaguchi, T.; Ohta, M.; Tsukamoto, S. Synthesis of 5-chloro-N-aryl-1H-indole-2-carboxamide derivatives as inhibitors of human liver glycogen phosphorylase a. *Bioorg. Med. Chem.*, **2008**, *16*, 5452-5464.

[42] Liu, G. X.; Zhang, Z. S.; Luo, X. M.; Shen, J. H.; Liu, H.; Shen, X.; Chen, K. X.; Jiang, H. L. Inhibitory mode of indole-2-carboxamide derivatives against HLGPa: molecular docking and 3D-QSAR analyses. *Bioorg. Med. Chem.*, **2004**, *12*, 4147-4157.

[43] Pinotsis, N.; Leonidas, D. D.; Chrysina, E. D.; Oikonomakos, N. G.; Mavridis, I. M. The binding of beta- and gamma-cyclodextrins to glycogen phosphorylase b: kinetic and crystallographic studies. *Protein Sci.*, **2003**, *12*, 1914-1924.

[44] Chen, L.; Li, H.; Liu, J.; Zhang, L.; Liu, H.; Jiang, H. Discovering benzamide derivatives as glycogen phosphorylase inhibitors and their binding site at the enzyme. *Bioorg. Med. Chem.*, **2007**, *15*, 6763-6774.

[45] Deng, Q.; Lu, Z.; Bohn, J.; Ellsworth, K. P.; Myers, R. W.; Geissler, W. M.; Harris, G.; Willoughby, C. A.; Chapman, K.; McKeever, B.; Mosley, R. Modeling aided design of potent glycogen phosphorylase inhibitors. *J. Mol. Graph. Model.*, **2005**, *23*, 457-464.

[46] Wen, X.; Zhang, P.; Liu, J.; Zhang, L.; Wu, X.; Ni, P.; Sun, H. Pentacyclic triterpenes. Part 2: Synthesis and biological evaluation of maslinic acid derivatives as glycogen phosphorylase inhibitors. *Bioorg. Med. Chem. Lett.*, **2006**, *16*, 722-726.

[47] Miller, M. D.; Sheridan, R. P.; Kearsley, S. K. SQ: a program for rapidly producing pharmacophorically relevent molecular superpositions. *J. Med. Chem.*, **1999**, *42*, 1505-1514.

[48] Lu, Z.; Bohn, J.; Bergeron, R.; Deng, Q.; Ellsworth, K. P.; Geissler, W. M.; Harris, G.; McCann, P. E.; McKeever, B.; Myers, R. W.; Saperstein, R.; Willoughby, C. A.; Yao, J.; Chapman, K. A new class of glycogen phosphorylase inhibitors. *Bioorg. Med. Chem. Lett.*, **2003**, *13*, 4125-4128.

[49] Catalyst, Accelrys Inc.: San Diego, CA.

[50] Wolber, G.; Langer, T. LigandScout: 3-D pharmacophores derived from protein-bound ligands and their use as virtual screening filters. *J. Chem. Inf. Model.*, **2005**, *45*, 160-169.

[51] Cheng, K.; Liu, J.; Liu, X.; Li, H.; Sun, H.; Xie, J. Synthesis of glucoconjugates of oleanolic acid as inhibitors of glycogen phosphorylase. *Carbohydr. Res.*, **2009**, *344*, 841-850.

[52] Kosmopoulou, M. N.; Leonidas, D. D.; Chrysina, E. D.; Eisenbrand, G.; Oikonomakos, N. G. Indirubin-3'-aminooxy-acetate inhibits glycogen phosphorylase by binding at the inhibitor and the allosteric site. Broad specificities of the two sites. *Lett. Drug Des. Discov.*, **2005**, *2*, 377-390.

[53] Furukawa, S.; Tsurumi, Y.; Murakami, K.; Nakanishi, T.; Ohsumi, K.; Hashimoto, M.; Nishikawa, M.; Takase, S.; Nakayama, O.; Hino, M. FR258900, a novel glycogen phosphorylase inhibitor isolated from Fungus No. 138354. I. Taxonomy, fermentation, isola-

tion and biological activities. *J. Antibiot. (Tokyo)* **2005**, *58*, 497-502.

[54] Tiraidis, C.; Alexacou, K. M.; Zographos, S. E.; Leonidas, D. D.; Gimisis, T.; Oikonomakos, N. G. FR258900, a potential anti-hyperglycemic drug, binds at the allosteric site of glycogen phosphorylase. *Protein Sci.*, **2007**, *16*, 1773-1782.

[55] Birch, A. M.; Kenny, P. W.; Oikonomakos, N. G.; Otterbein, L.; Schofield, P.; Whittamore, P. R.; Whalley, D. P. Development of potent, orally active 1-substituted-3,4-dihydro-2-quinolone glycogen phosphorylase inhibitors. *Bioorg. Med. Chem. Lett.*, **2007**, *17*, 394-399.

[56] Board, M.; Hadwen, M.; Johnson, L. N. Effects of novel analogues of D-glucose on glycogen phosphorylase activities in crude extracts of liver and skeletal muscle. *Eur. J. Biochem.*, **1995**, *228*, 753-761.

[57] Rath, V. L.; Ammirati, M.; LeMotte, P. K.; Fennell, K. F.; Mansour, M. N.; Danley, D. E.; Hynes, T. R.; Schulte, G. K.; Wasilko, D. J.; Pandit, J. Activation of human liver glycogen phosphorylase by alteration of the secondary structure and packing of the catalytic core. *Mol. Cell*, **2000**, *6*, 139-148.

[58] Hudson, J. W.; Golding, G. B.; Crerar, M. M. Evolution of allosteric control in glycogen phosphorylase. *J. Mol. Biol.*, **1993**, *234*, 700-721.

[59] Rath, V. L.; Ammirati, M.; Danley, D. E.; Ekstrom, J. L.; Gibbs, E. M.; Hynes, T. R.; Mathiowetz, A. M.; McPherson, R. K.; Olson, T. V.; Treadway, J. L.; Hoover, D. J. Human liver glycogen phosphorylase inhibitors bind at a new allosteric site. *Chem. Biol.*, **2000**, *7*, 677-682.

[60] Tsitsanou, K. E.; Skamnaki, V. T.; Oikonomakos, N. G. Structural basis of the synergistic inhibition of glycogen phosphorylase a by caffeine and a potential antidiabetic drug. *Arch. Biochem. Biophys.*, **2000**, *384*, 245-254.

[61] Ekstrom, J. L.; Pauly, T. A.; Carty, M. D.; Soeller, W. C.; Culp, J.; Danley, D. E.; Hoover, D. J.; Treadway, J. L.; Gibbs, E. M.; Fletterick, R. J.; Day, Y. S.; Myszka, D. G.; Rath, V. L. Structure-activity analysis of the purine binding site of human liver glycogen phosphorylase. *Chem. Biol.*, **2002**, *9*, 915-924.

[62] Archontis, G.; Watson, K. A.; Xie, Q.; Andreou, G.; Chrysina, E. D.; Zographos, S. E.; Oikonomakos, N. G.; Karplus, M. Glycogen phosphorylase inhibitors: a free energy perturbation analysis of glucopyranose spirohydantoin analogues. *Proteins*, **2005**, *61*, 984-998.

[63] Watson, K. A.; Chrysina, E. D.; Tsitsanou, K. E.; Zographos, S. E.; Archontis, G.; Fleet, G. W.; Oikonomakos, N. G. Kinetic and crystallographic studies of glucopyranose spirohydantoin and glucopyranosylamine analogs inhibitors of glycogen phosphorylase. *Proteins*, **2005**, *61*, 966-983.

[64] Simonson, T.; Archontis, G.; Karplus, M. Free energy simulations come of age: Protein-ligand recognition. *Acc. Chem. Res.*, **2002**, *35*, 430-437.

[65] Shoichet, B. K.; McGovern, S. L.; Wei, B.; Irwin, J. J. Lead discovery using molecular docking. *Curr. Opin. Chem. Biol.*, **2002**, *6*, 439-46.

[66] Joseph-McCarthy, D.; Baber, J. C.; Feyfant, E.; Thompson, D. C.; Humblet, C. Lead optimization *via* high-throughput molecular docking. *Curr. Opin. Drug Discovery Devel.*, **2007**, *10*, 264-274.

[67] Schrödinger Software Suite, Schrödinger, LLC, New York, NY.

[68] Friesner, R. A.; Banks, J. L.; Murphy, R. B.; Halgren, T. A.; Klicic, J. J.; Mainz, D. T.; Repasky, M. P.; Knoll, E. H.; Shelley, M.; Perry, J. K.; Shaw, D. E.; Francis, P.; Shenkin, P. S. Glide: a new approach for rapid, accurate docking and scoring. 1. Method and assessment of docking accuracy. *J. Med. Chem.*, **2004**, *47*, 1739-1749.

[69] Friesner, R. A.; Murphy, R. B.; Repasky, M. P.; Frye, L. L.; Greenwood, J. R.; Halgren, T. A.; Sanschagrin, P. C.; Mainz, D. T. Extra precision glide: docking and scoring incorporating a model of hydrophobic enclosure for protein-ligand complexes. *J. Med. Chem.*, **2006**, *49*, 6177-6196.

[70] Villoutreix, B. O.; Eudes, R.; Miteva, M. A. Structure-based virtual ligand screening: recent success stories. *Comb. Chem. High Throughput Screen.*, **2009**, *12*, 1000-1016.

[71] Sousa, S. F.; Fernandes, P. A.; Ramos, M. J. Protein-ligand docking: current status and future challenges. *Proteins*, **2006**, *65*, 15-26.

[72] Perola, E.; Walters, W. P.; Charifson, P. S. A detailed comparison of current docking and scoring methods on systems of pharmaceutical relevance. *Proteins*, **2004**, *56*, 235-49.

[73] Dias, R.; de Azevedo, W. F., Jr. Molecular docking algorithms. *Curr. Drug Targets*, **2008**, *9*, 1040-1047.

[74] Rarey, M.; Kramer, B.; Lengauer, T.; Klebe, G. A fast flexible docking method using an incremental construction algorithm. *J. Mol. Biol.*, **1996**, *261*, 470-489.

[75] Claussen, H.; Buning, C.; Rarey, M.; Lengauer, T. FLEXE: efficient molecular docking considering protein structure variations. *J. Mol. Biol.*, **2001**, *308*(2), 377-395.

[76] Jones, G.; Willett, P.; Glen, R. C.; Leach, A. R.; Taylor, R. Development and validation of a genetic algorithm for flexible docking. *J. Mol. Biol.*, **1997**, *267*, 727-748.

[77] Jones, G.; Willett P.; Glen, R. C. Molecular recognition of receptor sites using a genetic algorithm with a descriptor of solvation. *J. Mol. Biol.*, **1995**, *245*, 45-53.

[78] Morris, G. M.; Goodsell, D. S.; Halliday, R. S.; Huey, R.; Hart, W. E.; Belew, R. K.; Olson, A. J. Automated docking using a Lamarckian genetic algorithm and an empirical binding free energy function. *J. Comput. Chem.*, **1998**, *19*, 1639-1662.

[79] Huey, R.; Morris, G. M.; Olson, A. J.; Goodsell, D. S. A semiempirical free energy forcefield with charge-based desolvation. *J. Comput. Chem.*, **2007**, 28, 1145-1152.

[80] Morris, G. M.; Huey, R.; Lindstrom, W.; Sanner, M. F.; Belew, R. K.; Goodsell, D. S.; Olson, A. J. AutoDock4 and AutoDockTools4: Automated docking with selective receptor flexibility. *J. Comput. Chem.*, **2009**, *30*, 2785-2791.

[81] Ewing, T. J. A.; Makino, S.; Skillman, A. G.; Kuntz, I. D. DOCK 4.0: Search strategies for automated molecular docking of flexible molecule databases. *J. Comput.-Aided Mol. Des.* **2001**, *15*, 411-428.

[82] Cavasotto, C. N.; Singh, N. Docking and high throughput docking: Successes and the challenge of protein flexibility. *Curr. Comput.-Aided Drug Des.*, **2008**, *4*, 221-234.

[83] Sherman, W.; Day, T.; Jacobson, M. P.; Friesner, R. A.; Farid, R. Novel procedure for modeling ligand/receptor induced fit effects. *J. Med. Chem.*, **2006**, *49*, 534-553.

[84] Graves, A. P.; Shivakumar, D. M.; Boyce, S. E.; Jacobson, M. P.; Case, D. A.; Shoichet, B. K. Rescoring docking hit lists for model cavity sites: predictions and experimental testing. *J. Mol. Biol.*, **2008**, *377*, 914-934.

[85] Lyne, P. D.; Lamb, M. L.; Saeh, J. C. Accurate prediction of the relative potencies of members of a series of kinase inhibitors using molecular docking and MM-GBSA scoring. *J. Med. Chem.*, **2006**, *49*, 4805-4808.

[86] Polydoridis, S.; Leonidas, D. D.; Oikonomakos, N. G.; Archontis, G. Recognition of ribonuclease a by 3 '-5 '-pyrophosphate-linked dinucleotide inhibitors: A molecular dynamics/continuum electrostatics analysis. *Biophys. J.*, **2007**, *92*, 1659-1672.

[87] Huang, N.; Kalyanaraman, C.; Bernacki, K.; Jacobson, M. P. Molecular mechanics methods for predicting protein-ligand binding. *Phys. Chem. Chem. Phys.*, **2006**, *8*, 5166-5177.

[88] Aqvist, J.; Medina, C.; Samuelsson, J. E. A new method for predicting binding affinity in computer-aided drug design. *Protein Eng.*, **1994**, *7*, 385-391.

[89] Zhou, R. H.; Friesner, R. A.; Ghosh, A.; Rizzo, R. C.; Jorgensen, W. L.; Levy, R. M. New linear interaction method for binding affinity calculations using a continuum solvent model. *J. Phys. Chem. B*, **2001**, *105*, 10388-10397.

[90] Wall, I. D.; Leach, A. R.; Salt, D. W.; Ford, M. G.; Essex, J. W. Binding constants of neuraminidase inhibitors: An investigation of the linear interaction energy method. *J. Med. Chem.*, **1999**, *42*, 5142-5152.

[91] Raha, K.; Peters, M. B.; Wang, B.; Yu, N.; Wollacott, A. M.; Westerhoff, L. M.; Merz, K. M., Jr. The role of quantum mechanics in structure-based drug design. *Drug Discov. Today*, **2007**, *12*, 725-731.

[92] Senn, H. M.; Thiel, W. QM/MM Methods for Biomolecular Systems. *Angew. Chem., Int. Ed.*, **2009**, *48*, 1198-1229.

[93] Cho, A. E.; Guallar, V.; Berne, B. J.; Friesner, R. Importance of accurate charges in molecular docking: quantum mechanical/molecular mechanical (QM/MM) approach. *J. Comput. Chem.*, **2005**, *26*, 915-931.

[94] Raha, K.; Merz, K. M., Jr. Large-scale validation of a quantum mechanics based scoring function: predicting the binding affinity and the binding mode of a diverse set of protein-ligand complexes. *J. Med. Chem.*, **2005**, *48*, 4558-4575.

[95] Irwin, J. J.; Shoichet, B. K. ZINC--a free database of commercially available compounds for virtual screening. *J. Chem. Inf. Model.*, **2005**, *45*, 177-182.

[96] Grater, F.; Schwarzl, S. M.; Dejaegere, A.; Fischer, S.; Smith, J. C. Protein/ligand binding free energies calculated with quantum mechanics/molecular mechanics. *J. Phys. Chem. B*, **2005**, *109*, 10474-10483.

[97] Khandelwal, A.; Balaz, S. QM/MM linear response method distinguishes ligand affinities for closely related metalloproteins. *Proteins*, **2007**, *69*, 326-339.

[98] Khandelwal, A.; Balaz, S. Improved estimation of ligand-macromolecule binding affinities by linear response approach using a combination of multi-mode MD simulation and QM/MM methods. *J. Comput.-Aided Mol. Des.*, **2007**, *21*, 131-137.

[99] Khandelwal, A.; Lukacova, V.; Comez, D.; Kroll, D. M.; Raha, S.; Balaz, S. A combination of docking, QM/MM methods, and MD simulation for binding affinity estimation of metalloprotein ligands. *J. Med. Chem.*, **2005**, *48*, 5437-5447.

[100] Cramer, R. D.; Patterson, D. E.; Bunce, J. D. Comparative Molecular-Field Analysis (Comfa) .1. Effect of Shape on Binding of Steroids to Carrier Proteins. *J. Am. Chem. Soc.*, **1988**, *110*, 5959-5967.

[101] Leach, A. R.; Gillet, V. J.; Lewis, R. A.; Taylor, R. Three-dimensional pharmacophore methods in drug discovery. *J. Med. Chem.*, **2010**, *53*, 539-558.

[102] So, S. S.; Karplus, M. A comparative study of ligand-receptor complex binding affinity prediction methods based on glycogen phosphorylase inhibitors. *J. Comput.-Aided Mol. Des.*, **1999**, *13*, 243-258.

[103] So, S. S.; Karplus, M. Evaluation of designed ligands by a multiple screening method: Application to glycogen phosphorylase inhibitors constructed with a variety of approaches. *J. Comput.-Aided Mol. Des.*, **2001**, *15*, 613-647.

[104] Bohm, H. J. The development of a simple empirical scoring function to estimate the binding constant for a protein ligand complex of known 3-dimensional structure. *J. Comput.-Aided Mol. Des.*, **1994**, *8*, 243-256.

[105] Bohm, H. J. The Computer-Program Ludi - a New Method for the Denovo Design of Enzyme-Inhibitors. *J. Comput.-Aided Mol. Des.*, **1992**, *6*, 61-78.

[106] Bohm, H. J. LUDI: rule-based automatic design of new substituents for enzyme inhibitor leads. *J. Comput.-Aided Mol. Des.*, **1992**, *6*, 593-606.

[107] Sutherland, J. J.; O'Brien, L. A.; Weaver, D. F. A comparison of methods for modeling quantitative structure-activity relationships. *J. Med. Chem.*, **2004**, *47*, 5541-5554.

[108] So, S. S.; Karplus, M. Evolutionary optimization in quantitative structure-activity relationship: An application of genetic neural networks. *J. Med. Chem.*, **1996**, *39*, 1521-1530.

[109] So, S. S.; Karplus, M. Genetic neural networks for quantitative structure-activity relationships: improvements and application of benzodiazepine affinity for benzodiazepine/GABAA receptors. *J. Med. Chem.*, **1996**, *39*, 5246-5256.

[110] So, S. S.; Karplus, M. Three-dimensional quantitative structure-activity relationships from molecular similarity matrices and genetic neural networks. 1. Method and validations. *J. Med. Chem.*, **1997**, *40*, 4347-4359.

[111] So, S. S.; Karplus, M. Three-dimensional quantitative structure-activity relationships from molecular similarity matrices and genetic neural networks. 2. Applications. *J. Med. Chem.*, **1997**, *40*, 4360-4371.

[112] Hahn, M. Receptor surface models. 1. Definition and construction. *J. Med. Chem.*, **1995**, *38*, 2080-2090.

[113] Hahn, M.; Rogers, D. Receptor surface models. 2. Application to quantitative structure-activity relationships studies. *J. Med. Chem.*, **1995**, *38*, 2091-2102.

[114] Kollman, P. Free-Energy Calculations - Applications to Chemical and Biochemical Phenomena. *Chem. Rev.*, **1993**, *93*, 2395-2417.

[115] Desmond Molecular Dynamics System, version 2.2, D.E. Shaw Research, New York, NY, 2009. Maestro-Desmond Interoperability Tools, version 2.2, Schrödinger LLC, New York, NY, **2009**.

[116] Bowers, K. J.; Chow, E.; Xu, H.; Dror, R. O.; Eastwood, M. P.; Gregersen, B. A.; Klepeis, J. L.; Kolossvary, I.; Moraes, M. A.; Sacerdoti, F. D.; Salmon, J. K.; Shan, Y.; Shaw, D. E. In: *Scalable Algorithms for Molecular Dynamics Simulations on Commodity Clusters* In: Proceedings of the ACM/IEEE Conference on Supercomputing (SC06), Tampa, Florida, November 11-17, **2006**.

[117] Alexacou, K. M.; Hayes, J. M.; Tiraidis, C.; Zographos, S. E.; Leonidas, D. D.; Chrysina, E. D.; Archontis, G.; Oikonomakos, N. G.; Paul, J. V.; Varghese, B.; Loganathan, D. Crystallographic and computational studies on 4-phenyl-N-(beta-D-glucopyranosyl)-1H-1,2,3-triazole-1-acetamide, an inhibitor of glycogen phosphorylase: comparison with alpha-D-glucose, N-acetyl-beta-D-glucopyranosylamine and N-benzoyl-N'-beta-D-glucopyranosyl urea binding. *Proteins*, **2008**, *71*, 1307-1323.

[118] Still, W. C.; Tempczyk, A.; Hawley, R. C.; Hendrickson, T. Semianalytical treatment of solvation for molecular mechanics and dynamics. *J. Am. Chem. Soc.*, **1990**, *112*, 6127-6129.

[119] Martin, Y. C. Let's not forget tautomers. *J. Comput.-Aided Mol. Des.*, **2009**, *23*, 693-704.

[120] Pospisil, P.; Ballmer, P.; Scapozza, L.; Folkers, G. Tautomerism in computer-aided drug design. *J. Recept. Signal. Transduct. Res.*, **2003**, *23*, 361-371.

[121] Milletti, F.; Storchi, L.; Sforna, G.; Cross, S.; Cruciani, G. Tautomer enumeration and stability prediction for virtual screening on large chemical databases. *J. Chem. Inf. Model.*, **2009**, *49*, 68-75.

[122] Todorov, N. P.; Monthoux, P. H.; Alberts, I. L. The influence of variations of ligand protonation and tautomerism on protein-ligand recognition and binding energy landscape. *J. Chem. Inf. Model.*, **2006**, *46*, 1134-1142.

[123] Oellien, F.; Cramer, J.; Beyer, C.; Ihlenfeldt, W. D.; Selzer, P. M. The impact of tautomer forms on pharmacophore-based virtual screening. *J. Chem. Inf. Model.*, **2006**, *46*, 2342-2354.

[124] Hopfinger, A. J.; Reaka, A.; Venkatarangan, P.; Duca, J. S.; Wang, S. Construction of a virtual nigh throughput screen by 4D-QSAR analysis: Application to a combinatorial library of glucose inhibitors of glycogen phosphorylase b. *J. Chem. Inf. Comput. Sci.*, **1999**, *39*, 1151-1160.

[125] Venkatarangan, P.; Hopfinger, A. J. Prediction of ligand-receptor binding free energy by 4D-QSAR analysis: Application to a set of glucose analogue inhibitors of glycogen phosphorylase. *J. Chem. Inf. Comput. Sci.*, **1999**, *39*, 1141-1150.

[126] Venkatarangan, P.; Hopfinger, A. J. Prediction of ligand-receptor binding thermodynamics by free energy force field three-dimensional quantitative structure-activity relationship analysis: Applications to a set of glucose analogue inhibitors of glycogen phosphorylase. *J. Med. Chem.*, **1999**, *42*, 2169-2179.

[127] Zhou, P.; Li, Z. L. 3D-QSAR studies on glycogen phosphorylase inhibitors by flexible comparative molecular field analysis. *Sci. China Ser. B-Chem.*, **2007**, *50*, 568-573.

[128] Pastor, M.; Cruciani, G.; Clementi, S. Smart region definition: a new way to improve the predictive ability and interpretability of three-dimensional quantitative structure-activity relationships. *J. Med. Chem.*, **1997**, *40*, 1455-1464.

[129] Martins, J. P.; Barbosa, E. G.; Pasqualoto, K. F.; Ferreira, M. M. LQTA-QSAR: a new 4D-QSAR methodology. *J. Chem. Inf. Model.*, **2009**, *49*, 1428-1436.

[130] Lindahl, E.; Hess, B.; van der Spoel, D. GROMACS 3.0: a package for molecular simulation and trajectory analysis. *J. Mol. Model.*, **2001**, *7*, 306-317.

[131] Hopfinger, A. J.; Wang, S.; Tokarski, J. S.; Jin, B. Q.; Albuquerque, M.; Madhav, P. J.; Duraiswami, C. Construction of 3D-QSAR models using the 4D-QSAR analysis formalism. *J. Am. Chem. Soc.*, **1997**, *119*, 10509-10524.

[132] Verma, J.; Malde, A.; Khedkar, S.; Iyer, R.; Coutinho, E. Local indices for similarity analysis (LISA)-a 3D-QSAR formalism based on local molecular similarity. *J. Chem. Inf. Model.*, **2009**, *49*, 2695-2707.

[133] Gohlke, H.; Klebe, G. DrugScore meets CoMFA: adaptation of fields for molecular comparison (AFMoC) or how to tailor knowledge-based pair-potentials to a particular protein. *J. Med. Chem.*, **2002**, *45*, 4153-4170.

[134] Pitonak, M.; Riley, K. E.; Neogrady, P.; Hobza, P. Highly accurate CCSD(T) and DFT-SAPT stabilization energies of H-bonded and stacked structures of the uracil dimer. *Chem. Phys. Chem.*, **2008**, *9*, 1636-1644.

[135] Pluhackova, K.; Grimme, S.; Hobza, P. On the Importance of Electron Correlation Effects for the Intramolecular Stacking Geometry of a Bis-Thiophene Derivative. *J. Phys. Chem. A*, **2008**, *112*, 12469-12474.

[136] Oikonomakos, N. G.; Kosmopoulou, M. N.; Chrysina, E. D.; Leonidas, D. D.; Kostas, I. D.; Wendt, K. U.; Klabunde, T.; Defossa, E. Crystallographic studies on acyl ureas, a new class of glycogen phosphorylase inhibitors, as potential antidiabetic drugs. *Protein Sci.*, **2005**, *14*, 1760-1771.

[137] Li, J.; Liu, H.; Yao, X.; Liu, M.; Hu, Z.; Fan, B. Quantitative structure-activity relationship study of acyl ureas as inhibitors of human liver glycogen phosphorylase using least squares support vector machines. *Chemometr. Intell. Lab. Syst.*, **2007**, *87*, 139-146.

[138] ICM-pro, Molsoft LLC: San Diego, CA.

[139] Hoover, D. J.; Lefkowitz-Snow, S.; Burgess-Henry, J. L.; Martin, W. H.; Armento, S. J.; Stock, I. A.; McPherson, R. K.; Genereux, P. E.; Gibbs, E. M.; Treadway, J. L. Indole-2-carboxamide inhibitors of human liver glycogen phosphorylase. *J. Med. Chem.*, **1998**, *41*, 2934-2938.

[140] Prathipati, P.; Pandey, G.; Saxena, A. K. CoMFA and docking studies on glycogen phosphorylase a inhibitors as antidiabetic agents. *J. Chem. Inf. Model.*, **2005**, *45*, 136-145.

[141] Zhang, L.; Li, H.; Zhu, Q.; Liu, J.; Chen, L.; Leng, Y.; Jiang, H.; Liu, H. Benzamide derivatives as dual-action hypoglycemic agents that inhibit glycogen phosphorylase and activate glucokinase. *Bioorg. Med. Chem.*, **2009**, *17*, 7301-7312.

[142] Matschinsky, F. M. Regulation of pancreatic beta-cell glucokinase: from basics to therapeutics. *Diabetes*, **2002**, *51*, S394-S404.

[143] Li, A. P. Screening for human ADME/Tox drug properties in drug discovery. *Drug Discov. Today*, **2001**, *6*, 357-366.

[144] Lin, J.; Sahakian, D. C.; de Morais, S. M. F.; Xu, J. H.; Polzer, R. J.; Winter, S. M. The role of absorption, distribution, metabolism, excretion and toxicity in drug discovery. *Curr. Top. Med. Chem.*, **2003**, *3*, 1125-1154.

[145] Yu, H. S.; Adedoyin, A. ADME-Tox in drug discovery: integration of experimental and computational technologies. *Drug Discov. Today*, **2003**, *8*, 852-861.

[146] Evans, K. A.; Li, Y. H.; Coppo, F. T.; Graybill, T. L.; Cichy-Knight, M.; Patel, M.; Gale, J.; Li, H.; Thrall, S. H.; Tew, D.; Tavares, F.; Thomson, S. A.; Weiel, J. E.; Boucheron, J. A.; Clancy, D. C.; Epperly, A. H.; Golden, P. L. Amino acid anthranilamide derivatives as a new class of glycogen phosphorylase inhibitors. *Bioorg. Med. Chem. Lett.*, **2008**, *18*, 4068-4071.

[147] Sparks, S. M.; Banker, P.; Bickett, D. M.; Carter, H. L.; Clancy, D. C.; Dickerson, S. H.; Dwornik, K. A.; Garrido, D. M.; Golden, P. L.; Nolte, R. T.; Peat, A. J.; Sheckler, L. R.; Tavares, F. X.; Thomson, S. A.; Wang, L.; Weiel, J. E. Anthranilimide-based glycogen phosphorylase inhibitors for the treatment of type 2 diabetes: 1. Identification of 1-amino-1-cycloalkyl carboxylic acid headgroups. *Bioorg. Med. Chem. Lett.*, **2009**, *19*, 976-980.

[148] Sparks, S. M.; Banker, P.; Bickett, D. M.; Clancy, D. C.; Dickerson, S. H.; Garrido, D. M.; Golden, P. L.; Peat, A. J.; Sheckler, L. R.; Tavares, F. X.; Thomson, S. A.; Weiel, J. E. Anthranilimide-based glycogen phosphorylase inhibitors for the treatment of Type 2 diabetes: 2. Optimization of serine and threonine ether amino acid residues. *Bioorg. Med. Chem. Lett.*, **2009**, *19*, 981-985.

[149] Onda, K.; Shiraki, R.; Ogiyama, T.; Yokoyama, K.; Momose, K.; Katayama, N.; Orita, M.; Yamaguchi, T.; Furutani, M.; Hamada, N.; Takeuchi, M.; Okada, M.; Ohta, M.; Tsukamoto, S. Design, synthesis, and pharmacological evaluation of N-bicyclo-5-chloro-1H-indole-2-carboxamide derivatives as potent glycogen phosphorylase inhibitors. *Bioorg. Med. Chem.*, **2008**, *16*, 10001-10012.

[150] Park, B. K.; Kitteringham, N. R. Effects of fluorine substitution on drug metabolism: pharmacological and toxicological implications. *Drug Metab. Rev.*, **1994**, *26*, 605-643.

[151] Hampson, L. J.; Arden, C.; Agius, L.; Ganotidis, M.; Kosmopoulou, M. N.; Tiraidis, C.; Elemes, Y.; Sakarellos, C.; Leonidas, D. D.; Oikonomakos, N. G. Bioactivity of glycogen phosphorylase inhibitors that bind to the purine nucleoside site. *Bioorg. Med. Chem.*, **2006**, *14*, 7835-7845.

[152] Beresford, A. P.; Segall, M.; Tarbit, M. H. In silico prediction of ADME properties: are we making progress? *Curr. Opin. Drug Discov. Devel.*, **2004**, *7*, 36-42.

[153] Gola, J.; Obrezanova, O.; Champness, E.; Segall, M. ADMET propertry prediction: the state of the art and current challenges. *QSAR Comb. Sci.*, **2006**, *25*, 1172-1180.

[154] Norinder, U.; Bergstrom, C. A. S. Prediction of ADMET properties. *Chem. Med. Chem.*, **2006**, *1*, 920-937.

[155] Lagorce, D.; Sperandio, O.; Galons, H.; Miteva, M. A.; Villoutreix, B. O. FAF-Drugs2: free ADME/tox filtering tool to assist drug discovery and chemical biology projects. *BMC Bioinformatics*, **2008**, *9*, 396.

[156] Villoutreix, B. O.; Renault, N.; Lagorce, D.; Sperandio, O.; Montes, M.; Miteva, M. A. Free resources to assist structure-based virtual ligand screening experiments. *Curr. Protein Pept. Sci.*, **2007**, *8*, 381-411.

[157] Mohan, C. G.; Gandhi, T.; Garg, D.; Shinde, R. Computer-assisted methods in chemical toxicity prediction. *Mini Rev. Med. Chem.* **2007**, *7*, 499-507.

[158] Lipinski, C. A. Drug-like properties and the causes of poor solubility and poor permeability. *J. Pharmacol. Toxicol. Methods* **2000**, *44*, 235-249.

[159] Lipinski, C. A.; Lombardo, F.; Dominy, B. W.; Feeney, P. J. Experimental and computational approaches to estimate solubility and permeability in drug discovery and development settings. *Adv. Drug Deliv. Rev.*, **1997**, *23*, 3-25.

[160] Veber, D. F.; Johnson, S. R.; Cheng, H. Y.; Smith, B. R.; Ward, K. W.; Kopple, K. D. Molecular properties that influence the oral bioavailability of drug candidates. *J. Med. Chem.*, **2002**, *45*, 2615-2623.

[161] Zamora, I.; Oprea, T.; Cruciani, G.; Pastor, M.; Ungell, A. L. Surface descriptors for protein-ligand affinity prediction. *J. Med. Chem.*, **2003**, *46*, 25-33.

[162] Cruciani, G.; Pastor, M.; Guba, W. VolSurf: a new tool for the pharmacokinetic optimization of lead compounds. *Eur. J. Pharm. Sci.*, **2000**, *11*(Suppl. 2), S29-S39.

[163] Cruciani, C.; Crivori, P.; Carrupt, P. A.; Testa, B. Molecular fields in quantitative structure-permeation relationships: the VolSurf approach. *Theochem*, **2000**, *503*, 17-30.

[164] Goodford, P. J. A Computational-Procedure for Determining Energetically Favorable Binding-Sites on Biologically Important Macromolecules. *J. Med. Chem.*, **1985**, *28*, 849-857.

[165] Juhasz, L.; Docsa, T.; Brunyaszki, A.; Gergely, P.; Antus, S. Synthesis and glycogen phosphorylase inhibitor activity of 2,3-dihydrobenzo[1,4]dioxin derivatives. *Bioorg. Med. Chem.*, **2007**, *15*, 4048-4056.

[166] Mannhold, R.; Poda, G. I.; Ostermann, C.; Tetko, I. V. Calculation of molecular lipophilicity: State-of-the-art and comparison of log P methods on more than 96,000 compounds. *J. Pharm. Sci.*, **2009**, *98*, 861-893.

[167] Hewitt, M.; Cronin, M. T. D.; Enoch, S. J.; Madden, J. C.; Roberts, D. W.; Dearden, J. C. In Silico Prediction of Aqueous Solubility: The Solubility Challenge. *J. Chem. Inf. Model.*, **2009**, *49*, 2572-2587.

[168] Kenny, P. W.; Sadowski, J. In: *Methods and Principles in Medicinal Chemistry*; Wiley-VCH: Weinheim, **2005**; Vol. *23*, pp. 271-285.

[169] Birch, A. M.; Kenny, P. W.; Simpson, I.; Whittamore, P. R. Matched molecular pair analysis of activity and properties of glycogen phosphorylase inhibitors. *Bioorg. Med. Chem. Lett.*, **2009**, *19*, 850-853.

[170] Erickson, J. A.; Jalaie, M.; Robertson, D. H.; Lewis, R. A.; Vieth, M. Lessons in molecular recognition: the effects of ligand and protein flexibility on molecular docking accuracy. *J. Med. Chem.*, **2004**, *47*, 45-55.

[171] Huang, S. Y.; Zou, X. Ensemble docking of multiple protein structures: considering protein structural variations in molecular docking. *Proteins*, **2007**, *66*, 399-421.

[172] Barril, X.; Morley, S. D. Unveiling the full potential of flexible receptor docking using multiple crystallographic structures. *J. Med. Chem.*, **2005**, *48*, 4432-4443.

[173] McCammon, J. A. Target flexibility in molecular recognition. *Biochim. Biophys. Acta*, **2005**, *1754*, 221-224.

[174] Li, X.; Cheng, T.; Liu, Z.; Wang, R. Evaluation of the performance of four molecular docking programs on a diverse set of protein-ligand complexes. *J. Comput. Chem.* **2010**, *31*, 2109-2125.

Received: March 31, 2010 Revised: July 02, 2010 Accepted: July 15, 2010